

In the reply, the referee's comments are in *italics*, our response is in normal text, and quotes from the manuscript are in [blue](#).

***Anonymous Referee #1***

*General comments*

*This paper presents the first analysis of the Himalayan glacier response to solar geoengineering, analyzing the response to a number of scenarios of future greenhouse gas emissions and stratospheric aerosol geoengineering. The authors employ a mixed empirical / statistical model of glacier change driven by temperature change alone and use statistical down-scaling of the GeoMIP multi-model ensemble to produce the input data for their model. They find that solar geoengineering could slow the rate of retreat of Himalayan glaciers and that this benefit would be lost were solar geoengineering to be terminated.*

*This study is a novel contribution to the geoengineering literature and addresses an important issue; however, there are a number of shortcomings in the study that need to be addressed.*

*Most importantly, the method employed by the authors excludes precipitation which is the most critical climate difference between scenarios which include solar geoengineering and those which don't. Studies have reported substantial reductions in monsoon precipitation in scenarios which include solar geoengineering and so it seems odd to exclude this from the analysis. The authors note that excluding precipitation will likely mean that their estimate of the efficacy of solar geoengineering is an overestimate but it is not clear the magnitude of this overestimate; is it of order 1%, 10%, 100%?*

*I'd strongly recommend that the authors either reintroduce precipitation back into their methodology (the model described can use precipitation but it was excluded) even if this is only to provide a robust sensitivity estimate that justifies its exclusion, and I'd suggest doing this even if there are serious shortcomings in the down-scaling method for precipitation or other methodological concerns. Failing that, a much more detailed justification for excluding precipitation should be made along with some robust regional estimates of the significance that the changes in precipitation should be expected to have. The authors note that Rupper and Roe (2008) calculated zonal-mean sensitivities of SMB to temperature and precipitation; I suggest using these to estimate the sensitivity. This study should make clear what the research needs are to make a better estimate of the effects of solar geoengineering on Himalayan glaciers and the significance of including precipitation is a critical question that this paper does not address well.*

**Reply:** In the revision, we include precipitation in our methodology and consider its impact on glacier change. We used zonal-mean sensitivities of SMB to temperature and precipitation calculated by Rupper and Roe (2008). We have done the simulations with precipitation using all models under all the scenarios.

We also add a whole new section on the uncertainties in the projections (section 5) and on the method validation section 3.3.

*I had a number of questions about the validity of the methodology adopted in this study*

*that either require the authors to change the methodology, present some additional justification for their approach, or provide some sense of the sensitivity of their approach to these issues. I list the most significant ones here but there are other minor concerns listed afterwards.*

*First, the authors make comparisons between the responses of a changing ensemble of models for different experiments. It is unclear how much of the difference between these experiment-ensemble means is due to the changing make-up of the ensembles and how much due to robust differences in response. This is particularly concerning in the case of G4 where the models produced very different temperature responses due to their differing treatments of the 5Tg of injected SO<sub>2</sub>.*

**Reply:** In the revision, we have done all the simulations using every GCM ensemble member and ensemble-mean under every climate scenario. We list the result by every model under all the scenarios in Table 4 in the revision. We also test the significance of the ensemble member differences.

Volume loss using the climate projected by HadGEM2-ES under G4 is far less than that by other models (Table 4), so we exclude it when calculating the G4 model mean.

We tested the differences between RCP8.5, RCP4.5 and G4 using the 4 models in common (Table 4), and find the glacier responses are significantly different ( $p < 0.05$ ). Although there are too few models in common between G3 and G4, the dominant influence of summer melting to the mass balance (Zhao et al., 2016), and the clear difference in temperature across HMA between G3 and G4 (Figs. 2,3) suggest the glacier response in HMA is different between G3 and G4.

*Second, the authors don't do enough to validate their approach. A comparison against historical data or a more explicit reference to studies which validate this approach is needed. Does this model predict stable, growing or shrinking glacier mass for pre-industrial climate conditions? Is this model in agreement with other similar models?*

**Reply:** Our model estimates were already discussed in comparison with estimates for RCP8.5 and 4.5 by Radić et al. (2014) and Marzeion et al. (2012) in the conclusion section of previous manuscript, and we also have them in Section 5.2 of the revision. This is the first simulation of geoengineering forcing of HMA glaciers.

In our method, we need to use glacier outline and glacier surface elevation to estimate glacier mass balance. Because we do not have such input data for the pre-industrial period, we cannot do simulations of glacier change for pre-industrial climate conditions.

In the revision, we added a new Section 3.3 which is about validation of the glacier model.

### 3.3 Validation of the glacier model and methodology

In this section we justify the selection of various parameter values used in the method here. In section 5 we indicate how elements in the model and climate forcing affect the uncertainties of the results we produce in section 4, and how those results compare with previous estimates of glacier evolution in HMA.

A crucial parameterization concerns the SMB-altitude gradients. The field data

(Table 1) include three more glaciers than those used in Zhao et al. (2014; 2016), and include a benchmark glacier from almost every sub-region. With so few glacier observations available, there is an issue of how representative they are of the general population. For inner Tibet, there are three glaciers (Zhadang, Gurenhekou and Xiao Dongkemadi Glacier) with SMB observations, and they have almost the same SMB-altitude gradients,  $0.0041 \text{ m m}^{-1}$ , over their common elevation range (5515~5750 m, Table 1); two glaciers (Naimona'nyi and Kangwure) in central Himalaya have SMB gradients of  $0.0038 \text{ m m}^{-1}$  in their common altitude range of 5700~6100 m. These similarities suggest that the measured glaciers share some important characteristics with the vast majority which are not surveyed.

Next we consider the choices for the initial value of ELA at the start year, different V-A scaling parameters and different ELA sensitivities to summer mean temperature and annual precipitation.

In choosing the initial ELAs for each glacier, there are several reasonable alternatives (Zhao et al., 2016): i) using ELAs interpolated from the first Chinese glacier inventory, ii) median elevations from RGI dataset, iii) the elevation of the 60th percentile of the cumulative area above the glacier terminus. These three choices lead to a range of about 2.5 mm of global sea level in glacier volume loss at 2050. In this study, we use median elevations from RGI dataset, which corresponds to the median result.

Zhao et al. (2014) showed that different volume-area scaling parameterizations can lead to  $\pm 5\%$  range of glacier volume loss. The set of parameters we use in this study corresponds to the lower bound of estimated volume loss, but one that is best matched to the observational dataset of 230 separate glaciers (Moore et al., 2013).

For the ELA sensitivity to summer mean temperature and annual precipitation, we use the zonal mean values from energy-balance modelling of glaciers in HMA by Rupper and Roe (2008). Alternatively, it can be estimated using an empirical formula for ablation and a degree-day method (Zhao et al., 2016). Zhao et al. (2016) calculated the ELA for nine glaciers in China, India and Kyrgyzstan, and compared them with the observed ELA time series by similarities of decadal trends and also annual variability. The Rupper and Roe ELA parameterization produced the best fits to observed ELA decadal trends on 9 glaciers, with a correlation coefficient of 0.6 which is significant ( $p < 0.05$ , the values we give for  $p$  are single tailed Pearson correlation tests).

Combining the above uncertainties would require a Monte Carlo simulation since the parameters combine non-linearly to produce glacier volume and area change; this is prohibitively expensive to perform given that a single simulation of all glaciers in HMA requires about 60 cpu hours on an 8 cores computer with parallel computing in Matlab. We did estimate elevation changes for individual glaciers directly from simulated volume and area changes, then calculated the average rate of elevation change for all the glaciers in each sub-region and compared them with remote-sensing estimates from 2003 to 2009 from Gardner and others (2013), Table 2. The correlation coefficient between the Gardner et al. (2013) estimates for the 6 RGI 5.0 sub-regions with data regional and our modeled regional averages is 0.7 which is marginally significant, ( $p < 0.1$ ).

In our simulations we have used constant lapse rates for temperature ( $0.65^\circ\text{C}/100$

m) and precipitation (3%/100 m). To check how reliable this is we chose 5 meteorological stations close to glaciers and calculated correlation coefficients for JJA temperature and annual precipitation at the station and at the nearest downscaled grid point from 1980 to 2013 (n=34). Precipitation correlations were higher than 0.85 for all the stations ( $p < 0.001$ ), while temperatures correlations were 0.47-0.85 ( $p < 0.01$ ).

Finally we explored the sensitivity to the choice of dataset used to correct model bias in temperatures. In addition to using historical temperature from the CRU dataset, we also did the simulation using temperature from Berkeley Earth project ( $0.5^\circ \times 0.5^\circ$  resolution; Rohde et al., 2013; <http://berkeleyearth.org/data/>). That simulation was done using temperature alone as the glacier driver, so precipitation for each glacier was constant over time. The simulated climate ensemble mean forced volume losses in the period 2010-2069 were +4% (G3), -9% (G4), -11% (RCP4.5) and -13% (RCP8.5) different from the results using the CRU dataset.

*Third, the authors need to fix parameters for the thousands of glaciers in their study area but only have 13 glaciers to base these parameters on. As they are making a regional analysis they use only the 3 nearest glaciers to fix parameters in a regional manner. It is not immediately clear how different these 13 glaciers are from the results presented and so it is not clear how sensitive the results are to this sampling. The authors don't discuss whether one could expect the sampled glaciers to be representative of their region or why one would expect robust regional differences between the glaciers' behavior.*

**Reply:** Although the number of sampled glaciers is only 13 and the glaciers are randomly located, we find interestingly that the SMB gradients of the few glaciers in one sub-region are similar in their common elevation range. Again in Section 3.3:

For inner Tibet, there are 3 glaciers (Zhadang, Gurenhekou and Xiao Dongkemadi Glacier) with SMB observations, and they have almost the same SMB-altitude gradients,  $0.0041 \text{ m m}^{-1}$ , over their common elevation range (5515~5750 m, Table 1); two glaciers (Naimona'nyi and Kangwure) in central Himalaya have SMB gradients of  $0.0038 \text{ m m}^{-1}$  in their common altitude range of 5700~6100 m. These similarities suggest that the measured glaciers share some important characteristics with the vast majority which are not surveyed.

In the revision, we improve Table 1 to make this clearer.

*Finally, the authors downscale temperature to a high-resolution grid however they don't make any assessment of whether this downscaled temperature data matches observations. I'd expect that there could be quite large differences between the real glacier altitude and the altitude of the nearest high-resolution grid point given the complex topography. I was also wondering given that the observed altitude of the glaciers is used to calculate the ELA, why not use it directly to perform this lapse-rate adjustment?*

**Reply:** We guess the referee did not get what we did in the data-downscaling. In fact, we did the lapse-rate adjustment for temperature data just as the referee suggests. In the revision, we used temperature data from CRU and precipitation data from GPCC, which

have good reputation of the data quality. We have done many changes in Section 3.2 and 3.3 on downscaling that hopefully help clarify it:

The temperature and precipitation on each glacier were calculated by an altitude temperature lapse rate of  $0.65^{\circ}\text{C}/100\text{ m}$ , precipitation lapse rate of  $3\%/100\text{ m}$ , and the elevation difference of the glacier surface elevation relative to the nearest fine grid point.

In our simulations we have used constant lapse rates for temperature ( $0.65^{\circ}\text{C}/100\text{ m}$ ) and precipitation ( $3\%/100\text{ m}$ ). To check how reliable this is we chose 5 meteorological stations close to glaciers and calculated correlation coefficients for JJA temperature and annual precipitation at the station and at the nearest downscaled grid point from 1980 to 2013 ( $n=34$ ). Precipitation correlations were higher than 0.85 for all the stations ( $p<0.001$ ), while temperatures correlations were 0.47-0.85 ( $p<0.01$ ).

*Relatedly, I'd recommend that the authors broaden the uncertainties section into a proper discussion that covers the shortcomings of the methodology employed and discusses the sensitivity of the findings to various assumptions. A key question which should motivate the material in this section is – how would the glacier response in a model with a full surface mass balance treatment driven directly by high-resolution climate data differ?*

**Reply:** We do broaden the uncertainties section (see Section 5 in the revision) to discuss the uncertainties caused by climate forcing and by glacier model. In the revision, we use the relatively high resolution, monthly-mean gridded  $0.5^{\circ}\times 0.5^{\circ}$  temperature data from the CRU TS 3.24 dataset instead of the  $1^{\circ}\times 1^{\circ}$  temperature data from Berkeley Earth project, which was used before. We also discuss possible dynamic downscaling for the glacier model in section 5.1:

The models are also relatively coarsely gridded, certainly compared with the vast majority of glaciers, and so differences may be expected between statistically downscaled forcings based on lapse rates that we use here and that produced from high resolution dynamic climate model forcing.

we note that the distribution of meteorological stations in the study region is very sparse, especially in the northwest of this region (Liu and Chen, 2000). Therefore, both the CRU gridded data and data from models projections that we used in this study may have low accuracy for specific glacier regions. This has also implications for the use of very high resolution dynamic models; one such model simulated air temperatures and down-welling radiative fluxes well, but not wind speed and precipitation, producing unstable results when used with the CLM45 land model that simulated ground temperatures and snow cover (Luo et al., 2013). Explicit glacier atmospheric mass balance modelling (Mölg et al., 2013), a technique based on very high spatial and temporal resolution climate data (hourly and 60 m) was used on Zhadang glacier (Fig. 1, Table 1) with in-situ observations available, but not across the general expanse of the glaciated region; this study also noted the importance of wind speed to glacier mass balance in the region influenced by the Indian monsoon. Maussion et al., (2013) demonstrate that 10 km resolution dynamic modelling of the region can be done



successfully, and potentially can improve the precipitation modelling over the statistical downscaling methodology we employ here, though to date this is a reanalysis dataset with no prognostic simulations. Zhao et al. (2014 and 2016) used a 25 km resolution regional climate model RegCM3 to drive their simulations of glacier response to scenario A1B. By 2050 under A1B (which is intermediate between RCP4.5 and 8.5 in temperature rises), a sea level rise equivalent to 9.2 mm was projected from HMA. In comparison, our estimates are 11.1-12.5 mm for RC4.5 and 8.5 (Fig. 4).

*I had a few concerns about the structure and the focus of the paper that relate to the regional climate analysis. First, it seems strange to separate the regional climate analysis from the regional glacier analysis. Why not start with the whole-region analysis of climate and glacier response and then conduct a regional climate and glacier analysis afterwards? Second, Figures 2 and 3 seem of very little use as there are no cues on these plots to relate the results presented to the regional glacier analysis in figure 7. Given glacier response is calculated across the region or over sub-regions, I'd recommend doing a sub-regional-mean analysis as in figure 7 instead of including figures 2 and 3. This would also help to make clearer how significant excluding precipitation from the analysis was.*

**Reply:** Agreed.

Firstly, we change the structure of the result section (Section 4) as follows:

#### 4 Result

##### 4.1 Climate and glacier change across HMA

###### 4.1.1 Temperature and precipitation over HMA

###### 4.1.2 Glacier change across HMA

##### 4.2 Sub-regional climate and glacier changes

###### 4.2.1 Sub-regional temperature and precipitation change

###### 4.2.2 Sub-regional glacier changes

Secondly, we changed Fig. 2 and 3 to sub-regional analysis of temperature and precipitation (Fig. 3 in the revision), which are similar and have better connection to Fig. 7 --- the sub-regional analysis of glacier volume change.

*Finally, the conclusion needs to be revised as it presents a lot of new results and material, some of which are not appropriate for a conclusion.*

**Reply:** We rewrote the whole conclusion section 6, and moved some material to the Uncertainty section 5.

#### ***Specific comments***

*L18-21 – unclear sentence: 5 under G4 what?*

**Reply:** Changed to [five models under G4](#) and [six models under RCP4.5 and RCP8.5](#).

*L23-25 – I don't recall this point being made in the paper.*

**Reply:** We removed this point in the revision.

*L30-31 – This is a far-reaching general statement extrapolated from a specific scenario.*

*It holds for the specific case but not for the general case.*

**Reply:** We remove this sentence.

*L55 – delete hence*

**Reply:** Done.

*L55-57 – These are very different types of reasons and I don't see how the second matters.*

**Reply:** We rewrite this sentence as “the glaciers are affected by both the South Asian monsoon system and the westerly cyclonic systems, depending on specific location across the region, thus the region integrates the climate response to two important global circulation systems (Mölg et al., 2013).”

*L57-60 – Irvine et al. 2012 is a semi-empirical study and McCusker et al. discussed ice-sheet implications of their climate model results but did not simulate ice-sheet or sea-level response at all.*

**Reply:** We move Irvine et al. (2012) to the correct place. We change this sentence to “glacier responses to geoengineering scenarios has been limited to studies on global responses based on semi-empirical models (Moore et al., 2010; Irvine et al. 2012) or from simplified ice sheet responses (Irvine et al. 2009; Applegate et al., 2015) or implications of climate model (McCusker et al., 2015), with nothing to date on mountain glacier impacts.”

*L75 – “regions of newly defined regions of ” – fix*

**Reply:** modified to “defined regions of”.

*L86-89 – This sentence is unclear. Why is this simple? What issues could this pose?*

**Reply:** All the glacier outlines data are taken from RGI 5.0 dataset. The Second Chinese Glacier Inventory and the “Glacier Area Mapping for Discharge from the Asian Mountains” (GAMDAM) inventory provide data in certain regions in RGI 5.0. As the referee asked below, we improve this paragraph to make this meaning clear.

Notice the date of the data are different in different regions. And the date range for each region is short – a few years. So we take the same date for the glaciers in one region from the same data source. We do not think it would bring big issue. We add “Because the data range from one data source is only a few years” here in the revision.

The Randolph Glacier Inventory (RGI) database contains outlines of almost all glaciers and ice caps outside the two ice sheets (Arendt et al., 2015). Our study region covers HMA (26–46° N, 65–105° E), which corresponds to the defined regions of Central Asia, South Asia West and South Asia East in the RGI 5.0. According to the RGI 5.0, the study region contains a total of 94,000 glaciers and a glaciated area of about 110,000 km<sup>2</sup>. The RGI 5.0 data inside China are based on the Second Chinese Glacier Inventory (Guo et al., 2015), which provides glacier outlines from 2006–2010, except for some older outlines from the First Chinese Glacier Inventory where suitable imagery could not be found - mainly in southern and eastern Tibet (the S and E Tibet RGI 5.0 sub-

region), most of which were made in the 1970s. The RGI 5.0 data outside China are from the “Glacier Area Mapping for Discharge from the Asian Mountains” (GAMDAM) inventory (Nuimura et al., 2015) and nearly all come from 1999–2003 with images selected as close to the year 2000 as possible. Because the data range from each data source is only a few years, we take three reference years: 1980, 2009, and 2000, as start dates for our model simulations of glaciers in S and E Tibet, elsewhere in China, and outside China, respectively.

*L90-95 – This approach needs some justification and citations – why is it appropriate? Is this a widely accepted approach? Etc.*

**Reply:** Using median altitude as a proxy of ELA is a widely accepted approach (e.g. Nuimura et al., 2015).

We add this in the revision:

Following previous authors (Nuimura, 2015; Zhao et al., 2016), we use median altitude from RGI 5.0 for each glacier as a proxy for equilibrium line altitude (ELA).

The sensitivity is discussed in section 3.3

In choosing the initial ELAs for each glacier, there are several reasonable alternatives (Zhao et al., 2016): i) using ELAs interpolated from the first Chinese glacier inventory, ii) median elevations from RGI dataset, iii) the elevation of the 60th percentile of the cumulative area above the glacier terminus. These three choices lead to a range of about 2.5 mm of global sea level in glacier volume loss at 2050. In this study, we use median elevations from RGI dataset, which corresponds to the median result.

*L98-99 – What precisely is done? I believe this is explained in the next section, if so make that link explicit.*

**Reply:** The parameterizations of mass balance with altitude relative to the ELA is precisely written in Zhao et al. (2014). We add this reference here.

*Fig 1 + other lat-lon plots – It would help to make sense of the lat-lon plots if there was some frame of reference beyond the lat-lon coordinates. Would it be possible to mark the numbered regions (referred to later) with boxes or outlines in this figure and then over lay this outline in the other plots. This would make these subsequent figures much more useful. Or alter natively lose the lat-lon plots entirely and focus on the area-average means for the different regions shown here and assessed in figure 7.*

**Reply:** We focus on the area-average means for the different regions. As the referee suggested here and afterward, we change Fig. 2 and 3 (the spatial maps of temperature and precipitation) to sub-regional analysis of temperature and precipitation.

*L115-145 – Is there any validation of this modeling approach? If not this is a major shortcoming. 2 previous papers are cited; if they contain a validation of this approach that should be brought up and explained.*

**Reply:** Section 3.3 Validation of the glacier model. And Section 5.2 on uncertainties discuss these issues in detail and at length.



*L116-130 – Some sense of the sensitivity of the method to this sampling of glaciers is needed. I did not find the values in the table easy to read so I couldn't tell from looking at this how large the differences were; perhaps a figure would help to illustrate this. Can you be sure that these differences are systematic regional differences rather than the quirks of individual glaciers? Why not take the average over all glaciers rather than just the 3 nearest? These questions ought to be answered here or else citations which address these questions cited. This is another source of uncertainty in the model projections but it is unclear how large it is.*

**Reply:** We do not quite understand all the points in this question. Hopefully the changes in Section 3 make the method clearer, along with the cited reference to Zhao et al 2014. We tried to clarify our method, in section 3.3, in relation to mass balance gradients we show. The point on sensitivity to SMB, Zhao et al 2016, showed that it is important, but where the data allow the gradients to be checked within a sub-region, they agree very well between glaciers:

With so few glacier observations available, there is an issue of how representative they are of the general population. For inner Tibet, there are 3 glaciers (Zhadang, Gurenhekou and Xiao Dongkemadi Glacier) with SMB observations, and they have almost the same SMB-altitude gradients, 0.0041 m m<sup>-1</sup>, over their common elevation range (5515~5750 m, Table 1); two glaciers (Naimona'nyi and Kangwure) in central Himalaya have SMB gradients of 0.0038 m m<sup>-1</sup> in their common altitude range of 5700~6100 m. These similarities suggest that the measured glaciers share some important characteristics with the vast majority which are not surveyed.

*L140-144 – The justification for excluding precipitation here is incomplete (as it is in section 4). What matters is not the fractional precipitation change but rather the ratio of  $a \times dT$  to  $b \times dP$ . If you have the beta values it should be straightforward to make a rough calculation of  $b \times dP$  so that a comparison can be made. This issue is critical to address properly as your model cannot distinguish GHG from solar forcing (as it uses  $dT$  alone) and solar geoengineering has a distinct effect on precipitation.*

**Reply:** Agreed.

In the revision, we include precipitation.

*L146-189 – Is there a validation for this approach, i.e. do the down-scaled, lapse-rate adjusted reanalysis data match observational data?*

**Reply:** Yes. To validate the downscaled, lapse-rate adjusted reanalysis data, we choose 5 climate stations close to glaciers and calculated correlation coefficients for the station JJA temperature and annual precipitation and the nearest downscaled gridpoint from 1980 to 2013 (n=34). Precipitation correlation was higher than 0.85 for all the stations ( $p < 0.001$ ), while temperatures correlations were 0.47-0.85 ( $p < 0.01$ ).

In the revision, we now use the relatively high resolution, monthly-mean gridded 0.5° × 0.5° temperature data from CRU TS 3.24 dataset (Harris et al., 2014), instead of 1° × 1° temperature data from Berkeley Earth Project, because CRU has better reputation

of data quality control. We use  $0.5^{\circ} \times 0.5^{\circ}$  monthly total gridded precipitation data from the Global Precipitation Climatology Centre (GPCC) Total Full V7 dataset (Becker et al., 2013).

*L148 – “the beginning years” not clear*

**Reply:** We run the simulations for glacier change from the relevant start years (Section 2) to the year 2089.

*L150-151 – This sounds like you don’t believe them, explain the limits of this approach or rewrite this sentence.*

**Reply:** In the revision, we use temperature data from CRU instead of Berkeley Earth Project. So we rewrite this sentence as “From the start years to 2013, we use the relatively high resolution, monthly-mean gridded  $0.5^{\circ} \times 0.5^{\circ}$  temperature data from the CRU TS 3.24 dataset (Harris et al., 2014)”.

*L159 – “and THE INCREASE IN greenhouse gas forcing” rather than the total forcing relative to pre-industrial.*

**Reply:** Done.

*L159-161 – Here and elsewhere need to make it clear that different models had a very different temperature, etc. response to G4’s 5Tg.*

**Reply:** OK. We add this in the revision “The across model spread of temperatures under G4 is larger than under e.g. RCP4.5, (there are too few ensemble member models under G3 to see this) because of differences in how the aerosol forcing is handled, and each model has a different temperature response to the combined long and shortwave forcing (Yu et al., 2015).”

*L162 – No. Injection stops which means the aerosol forcing will decay rather than instantly disappear.*

**Reply:** OK. We delete “driven by forcing from RCP4.5 alone”.

*L171 – be more specific, e.g. resolutions of  $\sim 2$  degrees.*

**Reply:** We show the resolution in Table 2. We add “(Table 2)” here.

*L176 – Does the glacier not have an altitude of its own recorded somewhere? How large could the difference between the nearest grid-box and the glacier’s actual altitude be? I suspect this could be quite large. Has this been dealt with by other papers /methods? Is there any way to get a sense of this?*

**Reply:** We rewrite this sentence to make it clear. The individual glacier has its own altitude. There is difference between the nearest grid-box and the glacier’s actual altitude. The temperature and precipitation on each glacier were calculated by an altitude temperature lapse rate of  $0.65^{\circ}\text{C}/100\text{ m}$ , precipitation lapse rate of  $3\%/100\text{m}$ , and the elevation difference of the glacier surface elevation relative to the nearest fine gridpoint.

*L191-222 – Why is a regional analysis here? The regional analysis of the glacier response is made much later, it would seem sensible to present this material alongside that.*

**Reply:** We changed the structure of the paper in the revision.

*L191-222 – Some warning should be given about reading too much into the small scale “features” in these plots. These are artifacts of the ensemble average of mismatched, coarse model grids that have been downscaled – no individual model has the kind of spatial variation seen in figure 3a for example*

**Reply:** OK. But as the referee suggested, we changed Fig. 3 to sub-regional analysis.

*L193 – estimate = calculate.*

**Reply:** We change “estimate” to “calculate”.

*Figure 2 and throughout – It is not clear whether the differences plotted in this figure and in all other figures are due solely to differences in the response to the experiments as is implicitly assumed or whether the different make-ups of the ensembles used in each experiment has affected the results substantially. Some measure of this effect should be made.*

**Reply:** As the referee suggested, we changed Fig. 2 to sub-regional analysis (Fig. 3 in the revision).

There are 4 models in common under RCP8.5, RCP4.5 and G4. We tested the differences between RCP8.5, RCP4.5 and G4 using the 4 models in common (Table 4), and find the glacier responses are significantly different ( $p < 0.05$ ). There are only 2 common ensemble members (BNU-ESM, HadGEM2-ES) used in both G3 and G4, but we exclude HadGEM2-ES because this model gives a very different result from other models under G4. So there is only BNU-ESM in common under G3 and G4.

*Figure 2 and other map plots – The continuous color scale is hard to read, is it possible to use a banded scale or to add contour lines?*

**Reply:** As the referee suggested, we changed Fig. 2 from a map to a sub-regional line plot (Fig. 3 in the revision).

*Figure 2 and other map plots – I’d suggest removing the stippling. First, I’m skeptical whether the measure plotted is useful, i.e. does it really give a good sense of the robustness of the regional results? Second, looking at these plots the stippling is applied at a scale much finer than the resolution of the models that generated the results. Third, it’s entirely absent from some figures suggesting that the stippling code was not implemented appropriately.*

**Reply:** As the referee suggested, we changed Fig. 2 and Fig. 3 to sub-regional line plots (Fig. 3 in the revision).

*Figure 2 and 3 – Are these annual-mean or JJA-mean results?*

**Reply:** They are JJA-mean temperature in Figure 2 and annual precipitation in Figure 3.

*L197 and throughout – Are mean +/- standard deviation (which I presume these are) measures appropriate when the ensemble consists of only 4 models? Perhaps mean (min, max) may be more appropriate and informative.*

**Reply:** For simplicity we prefer to stick with standard deviations for the results, and it also means that we can remove outliers such as the G4 result of HadGEM2-ES. We add a new table (Table 4) in the revision to show all model results, and their mean +/- standard deviation under all the scenarios.

*Table 3 – I'd recommend adding much more information here and converting this into a figure which covers the full range of the model responses for each experiment across the different glacier regions. This would help to address my concern about the absence of precipitation from the simulations and the poor justification for why this was left out. Reporting the changes in precipitation in percentage change may help or else this could be combined with an estimate of the beta parameter for glacier sensitivity to precipitation (perhaps expressed as a fraction of the temperature response) to give a quantified estimate of how significant the precipitation response is. Without such information and given that precipitation is excluded from the glacier model I don't see why devoting a page to the precipitation response was necessary.*

**Reply:** In the revision, we include precipitation in the model.

*Figure 3 – These precipitation results seem to have been down-scaled, how was this done?*

**Reply:** we downscale both the CRU gridded temperature data, the GPCC gridded precipitation data and the climate model output to a grid based on a land surface topography having resolution of  $0.1126^{\circ} \times 0.1126^{\circ}$  using an altitude temperature lapse rate of  $0.65^{\circ}\text{C}/100\text{ m}$ , an altitude precipitation lapse rate of  $3\%/100\text{m}$ , and elevation difference of the fine grid relative to the climate model grid.

*L218 – “Precipitation change ratios”? not clear what this means.*

**Reply:** We no longer use this approach in the manuscript.

*L225 – “projections ensembles”?*

**Reply:** We change it to “projections”.

*L233-241 – How does these results compare to previously published results? Perhaps cite the work that made the initial analyses of G3 and G4.*

**Reply:** We cite a paper Yu et al. (2015) here, and change this sentence to “There are relative coolings of  $1.05^{\circ}\text{C}$  under G3 and  $0.76^{\circ}\text{C}$  under G4 compared with RCP4.5 during 2020-2069 across the whole region (Fig. 3). Yu et al. (2015) noted that G3 produced a relative cooling of  $0.58^{\circ}\text{C}$  and G4 of  $0.53^{\circ}\text{C}$  in globally averaged temperature over the 2030-2069 period.”

L233 – Should “and the highest rate” read “at the highest rate”?

**Reply:** Yes. We change it.

L238 – 1.7C over what period?

**Reply:** The temperature rise is over the period 2070-2089 relative to the period 2050-2069. We add the period in the revision.

L239-241 – *Why does this happen? Here and elsewhere more care should be taken to make clear that G4 produced very different forcing and hence temperature responses in the different models. Some evaluation of how effective G4 was at cooling the climate in different models should be made or reference should be made to a study which makes this analysis.*

**Reply:** We add the reason in the revision. This is due to G4 having a constant stratospheric aerosol injection rate of 5 Tg SO<sub>2</sub> per year, while G3 gradual ramps-up the aerosol so that about twice as much is needed by 2069, depending upon the sensitivity of the particular model to stratospheric sulphate aerosols. Hence, the radiative impact of terminating G3 is about twice as large as terminating G4, and the termination temperature signal is much more obvious in G3 than G4.

We made it clear that “The across model spread of temperatures under G4 is larger than under e.g. RCP4.5, (there are too few ensemble member models under G3 to see this) because of differences in how the aerosol forcing is handled, and each model has a different temperature response to the combined long and shortwave forcing (Yu et al., 2015).”

In Yu et al. (2015), they found “Over the period from 2030 to 2069, the global average SAT under rcp45 increased by  $0.81 \pm 0.21$  °C compared with the baseline (average over 2010–2029 under rcp45); while G4, the 40 year annual global mean SAT increased by  $0.28 \pm 0.31$  °C”. So the cooling effect is about 0.54°C. Therefore, we add this paragraph in the revision

“There are relative coolings of 1.05° C under G3 and 0.76° C under G4 compared with RCP4.5 during 2020-2069 across the whole region (Fig. 3). Yu et al. (2015) noted that G3 produced a relative cooling of 0.58° C and G4 of 0.53° C in globally averaged temperature over the 2030-2069 period.”

*Figure 4 – There is a suspicious degree of agreement between the models in panel d. These models presumably have quite different Transient climate response (TCR)s, surely there would be greater differences than this at the regional scale. Please cite some other work or present some evidence that this is not a processing error on your behalf.*

**Reply:** The plots in Fig. 4 (which is Fig.2 in the revision) show the average temperatures after grid-point by grid-point bias corrections. Ranges found are slightly smaller than the regional spread found by Yu et al. (2015) due to grid-point by grid-point bias correction we apply here. Under RCP8.5, temperature rises in HMA about 5 °C from the year 2020 to 2089 (panel d), which is higher than the global temperature rise of 3°C

over the same period (IPCC AR5). We do not think we made any error.

*Figure 5 – Here and elsewhere the comparison is not simply between different experiments but between different ensembles of models. Some assessment of the significance of this difference ought to be made. A similar line plot like this would be a good place to do so.*

**Reply:** We add the spread between ensemble members in this plot.

*Figure 5 – Rather than going into the spatial pattern of the precip response in figure 3 (which is not used) why not add 2 panels on the precip response to this line plot? Alter natively, do the regional-average analysis I suggested earlier.*

**Reply:** We add 2 panels on the precipitation response in the revision.

*L249 – “averaged over the grids” what does this mean?*

**Reply:** it means the averaged over the downscaled grid.

*L263-264 – Explain why this happens. I presume it’s because the most sensitive glaciers have already retreated / disappeared but this isn’t mentioned anywhere. I’m wondering idly whether an overall sensitivity could be calculated.*

**Reply:** Yes: The RCP4.5 and RCP8.5 scenarios produce similar continuous mass loss until approximately 2035 (Fig. 4a) mainly due to the similarity of temperatures projected by RCP4.5 and RCP8.5 in the period 2020-2035 (Fig. 2), and both show relatively slower loss rates after about the year 2050 probably because the most sensitive glaciers have already retreated before 2050.

*L269 – explain why  $G3 > G4$ .*

**Reply:**  $G3$  reduces glacier loss more than  $G4$ , which is due to stronger temperature cooling effect under  $G3$  (section 4.1.1). We add this in the revision.

*L270-280 – There is too much reporting of values and not enough explanation in this paragraph.*

**Reply:** We add Table 4 to show the result of all the models, and remove some values here.

*L283-284 – Is this area-volume relation surprising? Aren’t they explicitly linked in the model?*

**Reply:** It is not surprising. We add “as may be expected” and delete “quite”.

*Figure 7 – This regional break-down is great, however it is a shame that none of the previous results are presented on the same basis. This regional (and subregional) analysis is much more useful than the spatial maps shown elsewhere, could temperature and precipitation responses be plotted for these regions?*

**Reply:** In the revision, we add the temperature and precipitation responses in each subregion.



*L288-301 – Why isn't the regional climate analysis here with the regional glacier analysis.*

**Reply:** We have changed the structure of the result section.

*L303-359 – It is unclear what this section is for. I'd suggest reframing this as a regular discussion section and broadening its scope to cover all the shortcomings of this study.*

**Reply:** we did so in the revision.

*L304-306 – This sentence is unclear.*

**Reply:** We improve this sentence as “[Firstly, only 3 ESMs participated in G3 but 5 in G4 simply because doing the G3 experiment is difficult and time-consuming to set-up.](#)”

*L315-320 – why is this included? Your simulations excluded precipitation effects.*

**Reply:** We include precipitation in the revision.

*L328-333 – This paragraph is unclear, it is hard to follow the references.*

**Reply:** We rephrase this, and split the paragraph into 4 different ones in Section 3.3. The relevant 4 lines are now: [In choosing the initial ELAs for each glacier, there are several reasonable alternatives \(Zhao et al., 2016\): i\) using ELAs interpolated from the first Chinese glacier inventory, ii\) median elevations from RGI dataset, iii\) the elevation of the 60th percentile of the cumulative area above the glacier terminus. These three choices lead to a range of about 2.5 mm of global sea level in glacier volume loss at 2050. In this study, we use median elevations from RGI dataset, which corresponds to the median result.](#)

*L334-338 – This is also unclear.*

**Reply:** We delete this since we include precipitation in the revision.

*L339-342 – Does it? You have not shown the relative significance of precipitation to temperature in this study and table 3 only reports the area-average results which differ from the regional responses.*

**Reply:** We remove this sentence since we include precipitation in the revision.

*L339 – if A1B shows a significant trend then surely RCP 8.5 would too given their similarity?*

**Reply:** We remove this sentence since we include precipitation in the revision.

*L344-346 – This sentence is unclear and it's not clear which observational data is referred to here.*

**Reply:** changed to : [The set of parameters we use in this study corresponds to the lower bound of estimated volume loss, but one that is best matched to the observational dataset of 230 separate glaciers \(Moore et al., 2013\).](#)

*L350-352 – I'm not sure how useful this measure is given the shortcomings in the approach and the systematic over-estimation due to the exclusion of precipitation. Also, extending the simulations out to 2150 could give rise to the problem that your simple approach to uncertainty bounds would include negative glacier mass.*

**Reply:** we removed this measure in the revision.

*L361-end – Much of the material presented in this conclusion is new, why does this not appear earlier?*

**Reply:** we moved them to the uncertainty section (Section 5) before conclusion.

*L372 – why is G3 extreme? There are more extreme possibilities. This is an arbitrary scenario.*

**Reply:** we remove “extreme”.

*L383-385 – This is flatly wrong as written here. This result is scenario dependent. If a greater cooling were exerted by solar geoengineering more glaciers would be saved.*

**Reply:** Perhaps we were unclear, we changed the final paragraph to:

Although G3 keeps the average temperature from increasing in the geoengineering period, G3 only slows glacier shrinkage by about 50% relative to losses from RCP8.5. Approximately 72% of glaciated area remains at 2069 under G3 compared with about 30% for RCP8.5. The reason for the G3 losses is likely to be that the glaciers in HMA are not in equilibrium with present day climate, so simply stabilizing temperatures at early 21st century levels does not preserve them. To do that would require significant cooling, perhaps back to early 20th century levels. Achieving that cooling by sulphate aerosol injection may not be possible. The 5 Tg of SO<sub>2</sub> per year specified in G4 is about the same loading as a 1991 Mount Pinatubo volcanic eruption every 4 yr (Bluth et al., 1992). G3 requires increasing rates of injection, to 9.8 Tg for the BNU-ESM at 2069. As aerosol loading increases, its efficacy decreases as particles coalesce and fall out of the stratosphere faster, while also becoming radiatively less effective (Niemeier and Timmreck, 2015). This effect is so strong that it appears unfeasible to use sulphate aerosols to completely eliminate warming from scenarios such as RCP8.5. Greenhouse gas emissions would require very drastic reduction from present levels, and net negative emissions within the next few decades, to limit global temperature rises to 1.5 or 2°C (Rogelj, et al., 2015). If such targets were met, then it is conceivable that plausible quantities of sulphate aerosol geoengineering may be able to maintain 2020 temperatures throughout the 21st century. Even if this politically very difficult combination of drastic emission cuts and quite aggressive sulphate aerosol geoengineering were done, then our simulations suggest the disappearance of about 1/3 of the glaciated area in HMA by 2069 still cannot be avoided.

In the reply, the referee's comments are in *italics*, our response is in normal text, and quotes from the manuscript are in blue.

## ***Anonymous Referee #2***

*In this study, the authors propose to drive a minimal glacier model with GCM projections in the HMA region. The innovative part of the study is that they assess the impact of geoengineering on glacier changes, which is (as far as I am aware of) not discussed very often. However, the study suffers from the over-simplification of the glacier processes and from poor uncertainty assessments, two points which have to be addressed before considering publication.*

### ***General comments***

#### ***Glacier model***

*The glacier model used in this study is quite far behind today's standards (e.g. Marzeion et al., 2012, Huss and Hock, 2015). I list here the major issues that need to be addressed:*

- the model only considers changes in ELA with respect to summer temperature. They justify their choice by saying that most glaciers in the region are of the summer accumulation type (which is not proven) and that precipitation varies little over the entire HMA (which is a qualitative statement, and also probably not true for the sub-regions, as shown in Fig. 3). Precipitation has to be considered by the model, and not only summer precipitation: winter precipitation and the differentiation between liquid and solid precipitation has to be taken into account (in particular for the whole western and northern part of the study region, where precipitation is not falling in summer)*

**Reply:** Yes the model is relatively simple, but we note that data are limited in HMA so providing verification and calibration for more sophisticated models is problematic (See the new Section 5).

Specifically addressing the issues raised:

We considered the annual precipitation, and the differentiation between liquid and solid precipitation in the revision.

- the response time of glaciers has to be taken into account. This has to be parameterised in the volume-area scaling relation, as discussed by Marzeion et al., (2012) and Bahr et al., (2015).*

**Reply:** We take into account the response time of glaciers. We add response time in the volume-area scaling relation as in Marzeion et al., (2012) and present it in section 3.1.

- it is not clear to me how glaciers are supposed to grow in this model. Many glaciers in the HMA are currently growing or at least stagnating (without mentioning debris-covered glaciers), ad point which is not discussed in the study.*

**Reply:** We add in the method section 3.1 a description of how we deal with glaciers growing. Integrating the SMB over each glacier gives the mass balance, which is also the volume change rate, which is converted to an area change rate using volume–area scaling.

The set of glacier surface grid points is updated every year --- the number of the grid points that need to be removed or added is calculated using the area change rate while the elevation of the grid points is updated using SMB.

For advancing glaciers, we add grid points to the glacier surface grid, whose elevations are all supposed to be the glacier elevation minimum in the  $n+1$ <sup>th</sup> year,  $z_{\min}(n+1)$ , which is obtained as follows by assuming a constant glacier surface slope,

$$z_{\min}(n+1) = z_{\max}(n+1) + \frac{L(n+1)}{L(n)} \cdot (z_{\min}(n) - z_{\max}(n)), \quad (5)$$

where  $z_{\max}(n+1)$  denotes the glacier elevation maximum in the  $n+1$ <sup>th</sup> year. We also limited the maximal surface increase at any point on the glacier to 15 m above the initial elevation at the starting year. We chose to do this because the valley glacier is physically constrained from growing above the level of the surrounding mountain ridge and side-walls.

• *the calibration of the mass-balance (MB) gradients is extremely loose. If I understand well, the MB gradients are defined for one glacier with observations and then applied to the entire sub-region. By looking at Table 1 (where the MB gradients are described), it looks very unlikely that there is any reason for the local MG gradients (which contain arbitrary altitude thresholds and other local properties) to be representative for the region. Here I suggest to use either data-driven gradients (i.e. based on climate data) or even much simpler statistical gradients models which would be easier to cross-validate (see validation section below).*

**Reply:** The SMB gradients are data-based and come from the sparse dataset available, as described in Zhao et al. (2014), with some additional glaciers in this study. We add information about ELA and altitude ranges for each glacier in Table 1. We have only one glacier with SMB measurements in most sub-regions, so we cannot do cross-validate everywhere. However, interestingly, in a few sub-region where there are two or three glaciers, we found that the SMB gradients of these glaciers is very similar in their common altitude range. For inner Tibet, there are 3 glaciers (Zhadang, Gurenhekou and Xiao Dongkemadi Glacier) with SMB observations, and they have almost the same SMB-altitude gradients,  $0.0041 \text{ m m}^{-1}$ , over their common elevation range (5515~5750 m, Table 1); two glaciers (Naimona'nyi and Kangwure) in central Himalaya have SMB gradients of  $0.0038 \text{ m m}^{-1}$  in their common altitude range of 5700~6100 m. These similarities suggest that the measured glaciers share some important characteristics with the vast majority which are not surveyed.

#### *Validation and uncertainty assessment*

*The current approach to uncertainty assessment is not robust enough. Validation (i.e. comparison against observations) is quasi non-existent. I agree that given the few*

*number of observations, the task is not trivial. But especially in this case, it is recommended to make full use of all available data:*

- the authors could make use of cross-validation to assess the impact of interpolating the gradients on mass-balance (see e.g. Michaelsen, 1987)*

**Reply:** We add a section 3.3 that discusses validation for the glacier model. We show that the model produces significant correlations on decadal scales with observations, and also how the benchmark glaciers agree well on MB gradients where they can be compared. We also show in Table 2 how the elevation changes simulated compare with satellite altimetry estimates at a marginally significant level, but which is of course limited in accuracy by the few regions and gross averaging from the satellite data. Section 5 also discusses in depth how climate forcing and the glacier model affect the simulations.

- several recent publications made use of satellite observations to assess geodetic MB (e.g. volume changes) in HMA. This could serve as basis for a region-wide validation during the last decade, if only qualitative. See e.g. Huss and Hock (2015) who made use of the region-wide estimates of Gardner et al. (2013)*

**Reply:** We have a section about validation of glacier model (section 3.3) in the revision. We also estimated elevation changes for individual glaciers directly from simulated volume and area changes, then calculated the average rate of elevation change for all the glaciers in each sub-region and compared them with remote-sensing estimates from 2003 to 2009 from Gardner and others (2013), Table 2. The correlation coefficient between the Gardner et al. (2013) estimates for the 6 RGI 5.0 sub-regions with data regional and our modeled regional averages is 0.7 which is marginally significant, ( $p < 0.1$ ).

Also note ELA evolution is a key parameter in the method. As a validation of the method, Zhao et al. (2016) calculated the ELA for nine glaciers in China, India and Kyrgyzstan, and compared them with the observed ELA time series by similarities of decadal trends and also annual variability. The ELA parameterization produced reasonable fits to observed ELA decadal trends on 9 glaciers, with a correlation coefficient of 0.6 which is significant ( $p < 0.05$ , the values we give for  $p$  are single tailed Pearson correlation tests).

- the spread between the GCM ensemble members should also be discussed, as it probably impacts the results a lot.*

**Reply:** We add the simulation results using GCM ensemble members, and discuss the spread between them in the revision.

### ***Specific comments***

*Add uncertainty ranges to numbers in the abstract*

**Reply:** done.

*L50: add references to the summer-accumulation type statement (e.g. Fujita, 2008). Besides, it is highly speculative (and probably wrong) to say that all glaciers in HMA*

are "mainly" of this type. See the classifications by Rupper and Roe (2008) or the classification by Maussion et al., (2014), which shows that large parts of HMA are not of the summer accumulation type.

**Reply:** Yes. In contrast to glaciers in higher latitudes, many on the Tibetan Plateau are summer accumulation type (e.g. Fujita et al., 2000), that is both surface snow fall and melting occur overwhelmingly in the 3 summer months of June, July and August, with little mass gain or loss throughout the remaining 9 months of the year. However some glaciers, especially in the northwestern parts of HMA are winter accumulation type (Maussion et al., 2014).

*L85: I don't understand the need to use different inventories in this study. It seems much more consistent to stick to one, and give all the figures for the one judged more adapted.*

**Reply:** We only use Randolph Glacier Inventory (RGI) 5.0 for glacier outlines. But different parts of the region uses different sources. The RGI 5.0 data inside China are based on the Second Chinese Glacier Inventory (Guo et al., 2015), which provides glacier outlines from 2006–2010, except for some older outlines from the First Chinese Glacier Inventory where suitable imagery could not be found - mainly in southern and eastern Tibet (the S and E Tibet RGI 5.0 sub-region), most of which were made in the 1970s. The RGI 5.0 data outside China are from the “Glacier Area Mapping for Discharge from the Asian Mountains” (GAMDAM) inventory (Nuimura et al., 2015) and nearly all come from 1999–2003 with images selected as close to the year 2000 as possible.

*L90: please justify your choice of the median for the ELA proxy. What consequences does this choice have in the case of glaciers which are far from equilibrium, as it is the case in Eastern Himalaya?*

**Reply:** In Section 3.3 In choosing the initial ELAs for each glacier, there are several reasonable alternatives (Zhao et al., 2016): i) using ELAs interpolated from the first Chinese glacier inventory, ii) median elevations from RGI dataset, iii) the elevation of the 60th percentile of the cumulative area above the glacier terminus. These three choices lead to a range of about 2.5 mm of global sea level in glacier volume loss at 2050. In this study, we use median elevations from RGI dataset, which corresponds to the median result

Table 2 in the revision shows that our model indicates E. Himalaya is in the largest negative mass balance of the sub-regions, in agreement with Gardner et al., 2013.

Sub-regions	Gardner and others (2013)	Modelled
E Himalaya	-0.89±0.18	-1.51±0.59

*L99-100: rephrase*

**Reply:** done.

*Table 1: explain the gradients column in the legend, specify units*



**Reply:** The unit of SMB gradients is  $\text{m m}^{-1}$ . We add it in the legend.

*L120: reformulate “to calculate two or three SMB gradients with altitude”, which is unclear to me*

**Reply:** We change it to “We calculate no more than three SMB gradients using in-situ SMB measurements for every glacier in Fig.1 and Table 1. Following Zhao et al (2014), the SMB–altitude profile is constructed for every glacier by using its own ELA and these SMB gradients.”

*L125: volume area scaling must be extended with a relaxation time scale! See Marzeion et al., (2012) and Bahr et al., (2015).*

**Reply:** We add relaxation time scale in the volume-area scaling, the same as in Marzeion et al., (2012).

*L127: “by assuming all the decrease in area takes place in the lowest parts of the glacier”: but how do you deal with growing glaciers?*

**Reply:** We add how to deal with growing glaciers in the revision in Section 3.1 and see the answer to the first main point of the referee.

*L143: “relatively small (<10%).”: I wonder as to which percentage the authors would consider that the precipitation changes aren’t “relatively small” anymore. I personally find that 10% is quite a big deal.*

**Reply:** We considered precipitation in the revision and removed these words.

*L150: why not considering CRU (<https://crudata.uea.ac.uk/cru/data/hrg/>), which has a resolution of 0.5deg?*

**Reply:** We used CRU temperature data instead of Berkeley Earth Project in the revision, but compare the two results together in Section 3.3. That simulation was done using temperature alone as the glacier driver, so precipitation for each glacier was constant over time. The simulated climate ensemble mean forced volume losses in the period 2010-2069 were +4% (G3), -9% (G4), -11% (RCP4.5) and -13% (RCP8.5) different from the results using the CRU dataset.

*L166: how are they different?*

**Reply:** Yu et al. (2015), noted that was no significant change in surface temperatures after sulphate was injected in the GISS-E2-R model possibly due to the efficacy of SO<sub>2</sub> forcing being relatively small as compared to CO<sub>2</sub> forcing in the model. Neither do we also find a termination effect in GISS-E2-R under G3. Therefore, we not use any results from GISS-E2-R.

*At the end of the methods section the reader is left with many questions about how the calibration of the  $\alpha$  parameter is done, and how the uncertainties are handled in the study.*

**Reply:** In Section 3.3 we discuss the calibration. For the ELA sensitivity to summer

mean temperature and annual precipitation, we use the zonal mean values from energy-balance modelling of glaciers in HMA by Rupper and Roe (2008). Alternatively, it can be estimated using an empirical formula for ablation and a degree-day method (Zhao et al., 2016). Zhao et al. (2016) calculated the ELA for nine glaciers in China, India and Kyrgyzstan, and compared them with the observed ELA time series by similarities of decadal trends and also annual variability. The Rupper and Roe ELA parameterization produced the best fits to observed ELA decadal trends on 9 glaciers, with a correlation coefficient of 0.6 which is significant ( $p < 0.05$ , the values we give for  $p$  are single tailed Pearson correlation tests).

*Fig 2 Fig 3: please make a figure following today's standards. Add country borders or topography (or anything that helps for orientation). Consider using discrete levels instead of continuous colors. Are the anomalies for the entire year or just the summer season?*

**Reply:** We add country borders in Figure 1. As suggested by the other referee, we replaced Fig 2 and 3 with sub-regional line plot plots (the new Fig. 3 in the revision).

*Fig 5: add the spread between the ensemble members*

**Reply:** done.

*Fig 6: the uncertainty associated with the various ensemble members should also appear in the spread.*

**Reply:** done.

*L317: deep convection*

**Reply:** Changed.

*Conclusions: part of the conclusions should be extended and moved to the discussion (in particular the comparison with other studies).*

**Reply:** done.

*L368: specify what "close" means*

**Reply:** We delete "close" and write "The results projected by our method have higher means but smaller uncertainties than theirs, but do not differ significantly."

## References

- Bahr, D. B., Pfeffer, W. T. and Kaser, G.: A review of volume-area scaling of glaciers, *Rev. Geophys.*, 95–140, doi:10.1002/2014RG000470, 2015.
- Fujita, K. and Ageta, Y.: Effect of summer accumulation on glacier mass balance on the Tibetan Plateau revealed by mass-balance model, *J. Glaciol.*, 46(153), 244–252, doi:10.3189/172756500781832945, 2000.
- Gardner, A. S., Moholdt, G., Cogley, J. G., Wouters, B., Arendt, A. a, Wahr, J., Berthier, E., Hock, R., Pfeffer, W. T., Kaser, G., Ligtenberg, S. R. M., Bolch, T., Sharp, M. J., Hagen, J. O., van den Broeke, M. R. and Paul, F.: A Reconciled Estimate of Glacier

*Contributions to Sea Level Rise: 2003 to 2009*, *Science.*, 340(6134), 852–857, doi:10.1126/science.1234532, 2013.

Marzeion, B., Jarosch, a. H. and Hofer, M.: Past and future sea-level change from the surface mass balance of glaciers, *Cryosphere*, 6(6), 1295–1322, doi:10.5194/tc-6-1295-2012, 2012

Maussion, F., Scherer, D., Mölg, T., Collier, E., Curcio, J. and Finkelnburg, R.: Precipitation Seasonality and Variability over the Tibetan Plateau as Resolved by the High Asia Reanalysis\*, *J. Clim.*, 27(5), 1910–1927, doi:10.1175/JCLI-D-13-00282.1, 2014.

Michaelson, J.: Cross-validation in statistical climate forecast models, *J. Clim. Appl. Meteorol.*, 26(11), 1589–1600, doi:10.1175/1520-0450(1987)026 <1589:CVISCF> 2.0.CO; 2, 1987.

Rupper, S. and Roe, G.: Glacier Changes and Regional Climate: A Mass and Energy Balance Approach, *J. Clim.*, 21(20), 5384–5401, doi:10.1175/2008JCLI2219.1, 2008. Interactive comment on *Atmos. Chem. Phys. Discuss.*, doi:10.5194/acp-2016-830, 2016.

---

# Glacier evolution in high mountain Asia under stratospheric sulfate aerosol injection geoengineering

Liyun Zhao<sup>1,2</sup>, ~~Yang Yi~~<sup>1</sup> Yi Yang<sup>1</sup>, Wei Cheng<sup>1</sup>, Duoying Ji<sup>1,2</sup>, John C. Moore<sup>1,2,3</sup>

<sup>1</sup>College of Global Change and Earth System Science, Beijing Normal University,  
19 Xijiekou Wai St., Beijing, 100875, China

<sup>2</sup>Joint Center for Global Change Studies, Beijing, 100875, China

<sup>3</sup>Arctic Centre, University of Lapland, P.O. Box 122, 96101 Rovaniemi, Finland

Corresponding author: john.moore.bnu@gmail.com

## Abstract:

Geoengineering by stratospheric sulfate aerosol injection may help preserve mountain glaciers by reducing summer temperatures. We examine this hypothesis for the glaciers in High Mountain Asia using a glacier mass balance model driven by climate simulations from the Geoengineering Model Intercomparison Project (GeoMIP). The G3 and G4 schemes specify use of stratospheric sulphate aerosols to reduce the radiative forcing under the Representative Concentration Pathway (RCP) 4.5 scenario for the 50 years between 2020 and 2069, and for a further 20 years after termination of geoengineering. We estimate and compare glaciers volume loss for every glacier in the region using a glacier model based on ~~glacier~~ surface mass balance parameterization under climate projections from ~~3three~~ Earth System Models under G3, ~~5five models~~ under G4 and ~~6six models~~ under RCP4.5 and RCP8.5. The ensemble projections suggest that glacier shrinkage over the period 2010-2069 are equivalent to sea-level rises of  $9.0 \pm 1.6$  mm (G3),  $11.5 \pm 2.5$  mm (G4 excluding HadGEM2-ES),  $15.5 \pm 2.3$  mm (RCP 4.5) and  $18.5 \pm 1.7$  mm (RCP8.5). Although G3 keeps the summer mean average temperature from increasing in the geoengineering period, ~~but~~ G3 only slows glacier shrinkage by about 50% relative to losses from RCP8.5. Approximately 72% of glaciated area remains at 2069 under G3 compared with about 30% for RCP8.5. The termination of geoengineering at 2069 under G3 leads to sudden temperature rise of about  $1.7^{\circ}\text{C}$  to  $3^{\circ}\text{C}$  and corresponding increase in glacier retreat. Glacier volume in inner

~~Tibet and eastern Himalaya is least affected by greenhouse gas forcing, and also benefits the most from geoengineering. The ensemble mean projections suggest that glacier shrinkage over the period 2010–2069 are equivalent to sea level rises of 8.4 mm (G3), 10.7 mm (G4), 14.7 mm (RCP 4.5) and 16.8 mm (RCP8.5). After the termination of geoengineering, annual mean glacier volume loss rate for all the glaciers under G3 increases from 0.3917% a<sup>-1</sup> to 0.9011% a<sup>-1</sup>, which are higher than the 0.7066% a<sup>-1</sup> under RCP8.5 at that time. While sulphate aerosol injection geoengineering may slow glacier loss in the region, it cannot prevent about a third of existing glacier coverage disappearing by 2069 during 2070–2089.~~

**keywords:** sea level rise; mass balance; climate impacts

## 1. Introduction

High Mountain Asia (HMA) contains the largest number of glaciers outside the polar regions. These glaciers provide water for many large and important rivers (e.g. Brahmaputra, Ganges, Yellow, Yangtze, Indus, and Mekong), and most, but not all, have shrunk over recent decades (Yao et al., 2012). The response of these glaciers to future climate change is a topic of concern especially to the many people who rely on glacier-fed rivers for purposes such as irrigation.

Glacier evolution is expected to be sensitive to climate change. Temperature and precipitation are the important climate factors affecting glaciers. Geoengineering is a method of offsetting the global temperature rise from greenhouse gases, although inevitably also altering other important climate parameters, such as precipitation and global atmosphere and ocean circulation teleconnection patterns (Tilmes, et al., 2013; Ricke, et al., 2010). There have been various studies on mountain glacier change under future climate scenarios such as A1B, and the various Representative Concentration Pathway (RCP) scenarios (Marzeion et al., 2012; Radić et al., 2014; Zhao et al., 2014). In contrast to glaciers in higher latitudes, ~~those in HMA~~many on the Tibetan Plateau are ~~mainly~~ summer accumulation type, ~~(e.g. Fujita et al., 2000)~~, that is both surface snow fall and melting occur overwhelmingly in the 3 summer months of June, July and August, with little mass gain or loss throughout the remaining 9 months of the year.

~~The~~However some glaciers, especially in the northwestern parts of HMA are winter accumulation type (Maussion et al., 2014). Hence, the glaciers are affected by both the South Asian monsoon system and the westerly cyclonic systems, depending on specific location across the region. ~~Hence, thus~~ the region ~~is important both to people dependent on glacier water supplies, and because it~~ integrates the climate response to two important global circulation systems. ~~However, glacier~~ (Mölg et al., 2013).

Glacier responses to geoengineering scenarios has been limited to studies on global responses based on semi-empirical models (Moore et al., 2010; Irvine et al. 2012) or from simplified ice sheet responses (Irvine et al. 2009, 2012; McCusker; Applegate et al., 2015; Applegate) or implications of climate model (McCusker et al., 2015), with nothing to date on mountain glacier impacts.

In this paper, we predict glacier area and volume change for every glacier in HMA under ~~forcing by output~~projections from 6 Earth System Models (ESM) simulations of climate under the Geoengineering Model Intercomparison Project (GeoMIP) G3 and G4 scenarios (Kravitz et al., 2011). These scenarios envisage use of stratospheric sulphate aerosols to reduce the radiative forcing under the RCP 4.5 greenhouse gas scenario during in a 50 year period from 2020 to 2069 followed by sudden cessation of geoengineering to determine the “termination effect” (Jones et al., 2013) but continued RCP4.5 greenhouse gas forcing for a further 20 years. We address two questions here: (1) Would glacier shrinkage and loss in HMA be alleviated under geoengineering by stratospheric sulfate aerosol injection? (2) How would the glaciers respond to the termination of geoengineering?

## 2. Study region and glacier data

The Randolph Glacier Inventory (RGI) database contains outlines of almost all glaciers and ice caps outside the two ice sheets (Arendt et al., 2015). Our study region covers HMA (26–46 ° N, 65–105 ° E), which corresponds to the ~~regions of newly~~ defined regions of Central Asia, South Asia West and South Asia East in the ~~Randolph Glacier Inventory~~ (RGI) 5.0 ~~(Arendt et al., 2015).~~ According to the RGI RGI 5.0, the study



region contains a total of 94,000 glaciers and a glaciated area of about 110,000 km<sup>2</sup>. ~~To estimate how each of these glaciers change we require for each one a reference area and volume. Glacier area estimates~~The RGI 5.0 data inside China are based on the Second Chinese Glacier Inventory (Guo et al., 2015), which provides glacier outlines from ~~a target period of 2006–2010, but includes~~except for some older outlines from the First Chinese Glacier Inventory where suitable imagery could not be found ~~within the target period-~~ mainly in ~~the~~ southern and eastern Tibet (the S and E Tibet RGI 5.0 sub-region: Glacier outlines), ~~most of which were made in the 1970s. The RGI 5.0 data~~ outside China are from the “Glacier Area Mapping for Discharge from the Asian Mountains” (GAMDAM) inventory (Nuimura et al., 2015) and nearly all come from 1999–2003 with images selected as close to the year 2000 as possible. ~~Therefore, for simplicity~~Because the data range from each data source is only a few years, we take three reference years: 1980, 2009, and 2000, as ~~the reference years and start of dates for~~ our model simulations ~~for~~of glaciers ~~inside southern S and eastern E Tibet, inside elsewhere in China-expect southern and eastern Tibet~~, and outside China, respectively.

~~We~~Following previous authors (Nuimura, 2015; Zhao et al., 2016), we use median altitude from RGI 5.0 for each glacier as a proxy for equilibrium line altitude (ELA) in the respective initial years; that is the altitude on the glacier where the local net surface mass balance (SMB) is zero. We use the Shuttle Radar Topography Mission (SRTM) version 4.1 (void-filled version; Jarvis et al, 2008) digital elevation model with 90 m horizontal resolution to estimate the elevation range spanned by each glacier.

Field measurements on SMB are rare in the HMA due to difficulty of access to the glaciers. ~~Here~~Following Zhao et al. (2014), we collate SMB versus altitude measurements from 13 glaciers (Table 1 and Fig. 1), to set up parameterizations of mass balance with altitude relative to the ELA for all glaciers. ~~This field data are more than previously used in the model (Zhao et al., 2014; 2016), with a benchmark glacier in almost every sub-regions. With so few glacier observations available there is an issue of how representative they are of the general population. For inner Tibet, there are 3 glaciers (Zhadang, Gurenhekou and Xiao Dongkemadi Glacier) with SMB observations,~~

and they have almost the same value of SMB gradients in similar altitude ranges (Table 1); as so do the two glaciers (Naimona'nyi and Kangwure) in central Himalaya. These similarities suggest that at least the measured glaciers share some important characteristics with the vast majority which are not surveyed.

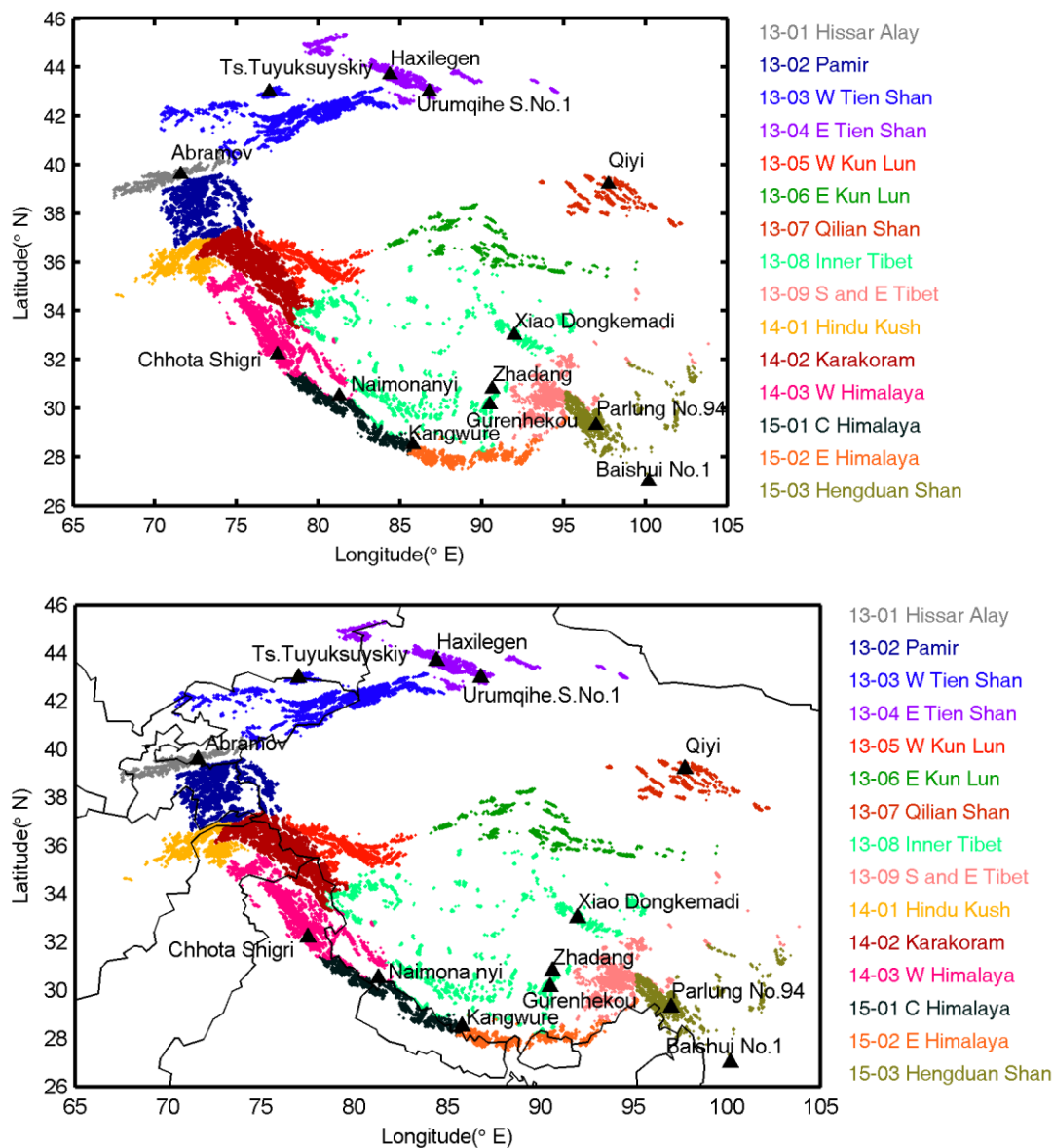


Fig. 1 The HMA region analyzed. Sub-regions of the HMA in RGI 5.0 are listed and colour-coded in the legend. The black curves represent the boundaries between regions 13 (Central Asia), 14 (South Asia West) and 15 (South Asia East). Glaciers with SMB measurements (Table 1) are marked with black triangles.

### 3. Methodology

#### 3.1 Statistical model of glacier change

The statistical model for estimating glacier change is based on Zhao et al (2014; 2016).

Briefly the algorithm can be described as follows. We start from known glacier outlines from RGI 5.0 and glacier elevation distribution from SRTM 4.1. In the start year, SRTM DEM data (90 m horizontal resolution) inside the glacier outline are interpolated onto a regular grid with a spatial resolution of 10 m covering the glacier surface. Vertical spacing of altitude bands depends on glacier size, taken as 10 m for glaciers with a total elevation difference from top to bottom larger than 100 m, and one tenth of the glacier altitude difference for glaciers with less altitude range.

We parameterize the annual SMB as a function of altitude relative to the ELA for each glacier. ~~We use the available~~ We calculate no more than three SMB gradients using in-situ SMB measurements on 13 glaciers (for every glacier in Fig. 1) to calculate two or three SMB gradients with altitude (and Table 1). ~~The.~~ Following Zhao et al (2014), the SMB–altitude profile is constructed for every glacier by using its own ELA and no more than three these SMB gradients. Where SMB data exists in the sub-region, we use them to parameterize the SMB of all glaciers in that sub-region. Otherwise, we use glaciers from nearby sub-regions.

Integrating the SMB over each glacier gives the volume change rate, which is converted to an area change rate using volume–area scaling. ~~The area change rate then gives the new glacier terminus position and hence the new outline for the next year by assuming all the decrease in area takes place in the lowest parts of the glacier. Combining the glacier elevation distribution, the SMB and the new outline, we obtain glacier elevation distribution for the next year.~~ (Marzeion et al., 2012)

$$dA(n+1) = \frac{1}{\tau_A} \left( \left( \frac{V(n+1)}{c_A} \right)^{1/\gamma} - A(n) \right) \quad (1)$$

where  $A(n)$  is glacier area in the  $n_{th}$  year,  $V(n+1)$ ,  $dA(n+1)$  are glacier volume and area change rate in the  $n+1_{th}$  year, respectively,  $c_A = 0.0380 \text{ km}^{3-2\gamma}$  and  $\gamma = 1.290$

(Moore et al., 2013),  $\tau_A$  is the response time scale of glacier area and calculated as

$$\tau_A(n) = \tau_L(n) \frac{A(n)}{L(n)^2} \quad (2)$$

where  $L(n)$  and  $\tau_L$  are glacier length and the response time scale of glacier length in the  $n$ th year, respectively.  $\tau_L$  is calculated by

$$\tau_L(n) = \frac{V(n)}{A(n) \cdot P^{solid}(n)} \quad (3)$$

following the scaling of Johannesson et al. (1989) where  $V(n)$  and  $P^{solid}(n)$  denote glacier volume and the solid precipitation on the glacier in the  $n$ th year, respectively. The initial glacier length  $L_{start}$  is estimated by area-length scaling  $A_{start} = c_L L_{start}^{q_L}$  where  $c_L = 0.0180 \text{ km}^{3-q}$  (Radic et al., 2008) and  $q = 2.2$  (Bahr et al., 1997). The glacier length change is calculated using the area-length scaling

$$dL(n+1) = \frac{1}{\tau_L} \left( \left( \frac{A(n+1)}{c_L} \right)^{1/q} - L(n) \right) \quad (4)$$

We assume all the area changes take place in the lowest parts of the glacier. The set of glacier surface grid points is updated every year --- the number of the grid points that need to be removed or added is calculated using the area change rate while the elevation of the grid points is updated using SMB.

For retreating glaciers, we remove grid cells near the glacier terminus from the glacier surface grids and get the new glacier terminus position and hence the new outline for the next year. For advancing glaciers, we add grid points to the glacier surface grid, whose elevations are all supposed to be the glacier elevation minimum in the  $n+1$ th year,  $z_{min}(n+1)$ , which is obtained as follows by assuming a constant glacier surface slope.

$$z_{min}(n+1) = z_{max}(n+1) + \frac{L(n+1)}{L(n)} \cdot (z_{min}(n) - z_{max}(n)) \quad (5)$$

where  $z_{\max}(n+1)$  denotes the glacier elevation maximum in the  $n+1$ th year. We also limited the maximal surface increase at any point on the glacier to 15 m above the initial elevation at the starting year. We chose to do this because the valley glacier is physically constrained from growing above the level of the surrounding mountain ridge and side-walls.

The SMB–altitude profile on each glacier is evolved annually as the ELA changes. And the ELA evolution is estimated by using its sensitivities with respect to temperature and precipitation as follows:

~~$$ELA_n = ELA_{n-1} + \alpha \Delta T + \beta \Delta P, \quad (1)$$~~

$$ELA_n = ELA_{n-1} + \alpha \Delta T + \beta \Delta P, \quad (6)$$

where  $ELA_n$  is the ELA in the  $n$ th year from the beginning year,  $\Delta T$  and  $\Delta P$  are the inter-annual change of summertime (June-July-August) mean air temperature and annual solid precipitation on the glacier, the coefficients  $\alpha$  (unit:  $m \text{ } ^\circ C^{-1}$ ) and  $\beta$  (unit:  $m \text{ } m^{-1}$ ) are the sensitivity of ELA shift to air temperature change ( $^\circ C$ ) and precipitation change (m), respectively, which are zonal mean values from energy-balance modelling of glaciers in HMA by Rupper and Roe (2008), see also Zhao et al. (2014). We show in Section 4, that simulated precipitation changes under all the climates we study here are relatively small ( $<10\%$ ). Therefore we choose to remove precipitation changes from our simulations of HMA glaciers, hence we assume that changes of ELA in Eqn (1) are controlled by summer temperature variation alone. (2014).

### 3.2 Climate scenarios and downscaling of climate data

We run the simulations for glacier change from the relevant start years (Section 2) to the year 2089. From the beginning start years to 2013, we use the relatively high resolution, daily monthly-mean gridded  $1^\circ \times 10.5^\circ \times 0.5^\circ$  temperature data from the Berkeley Earth project (Rohde CRU TS 3.24 dataset (Harris et al., 2014), and  $0.5^\circ \times 0.5^\circ$  monthly total gridded precipitation data from the Global Precipitation Climatology Centre (GPCC) Total Full V7 dataset (Becker et al., 2013; <http://berkeleyearth.org/data/>)

which are generated by supposedly using all available station data and a bespoke interpolation method).

~~We use the Coupled Model Intercomparison Project Phase 5 (CMIP5; Taylor, et al., 2012) output of all models.~~ For the years 2014 to 2089 we use 4 kinds of climate forcing: experiment RCP4.5, RCP8.5, and results from two GeoMIP scenarios (G3 and G4; Kravitz et al., 2011) which use stratospheric aerosols to reduce the incoming shortwave while applying the RCP4.5 greenhouse gas forcing. In G3 and G4, stratospheric geoengineering of sulphate aerosol injection starts in the year 2020 and ends in the year 2069. In the 50 years of geoengineering under G3 there is close to a balance between reduction of incoming shortwave radiation and the increase in greenhouse gas forcing, while G4 specifies continuous injection of SO<sub>2</sub> into the equatorial lower stratosphere at a rate of 5 Tg per year from 2020. The across model spread of temperatures under G4 is larger than under e.g. RCP4.5 (there are too few ensemble member models under G3 to see this) because of differences in how the aerosol forcing is handled, and each model has a different temperature response to the combined long and shortwave forcing (Yu et al., 2015). Following the abrupt end of geoengineering, both G3 and G4 specify 20 years of further simulation from 2070 to 2089 ~~driven by forcing from RCP4.5 alone.~~

We derived climate forcing data from 3three climate models participating in G3, 5 models in G4, 6six models in RCP4.5 and 6in RCP8.5 (Table 3). ~~We use the Coupled Model Intercomparison Project Phase 5 (CMIP5; Taylor, et al., 2012) output of all models.~~ Yu et al. (2015), ~~we~~ noted there was no significant change in surface temperatures after sulphate aerosol was injected in the GISS-E2-R model possibly due to the efficacy of SO<sub>2</sub> forcing being relatively small as compared to CO<sub>2</sub> forcing in the model. Neither do we also find a termination effect in GISS-E2-R under G3. Therefore, we not use any ~~GISS-E2-R~~ results ~~here because its projected fields are very different~~ from ~~other models~~ GISS-E2-R. We also exclude the model CISRO-Mk3L due to its very coarse spatial resolution of about 4° and 4° and the absence of simulation ~~result~~ results in the year 2020 under G4; the models used and their resolutions are listed in Table 23.

Compared with the size of most glaciers in HMA (typically km scale), ~~both~~ the



~~Berkeley grids~~CRU, GPCC and climate ~~models~~model grids have rather coarse resolution- (Table 3). The direct use of coarse grid points naturally results in a poor representation of the local climate. Hence we downscale both the ~~Berkeley~~CRU gridded ~~temperature data, the GPCC gridded precipitation~~ data and the climate ~~models~~model output to a grid based on a land surface topography having resolution of  $0.1126^\circ \times 0.1126^\circ$  using an altitude temperature lapse rate of  $0.65^\circ\text{C}/100\text{ m}$ , ~~an altitude precipitation lapse rate of 3%/100 m~~, and elevation difference of the fine ~~local~~ grid ~~point~~ relative to the climate model grid. ~~For each individual glacier, we use the data at the grid nearest to this glacier to represent the local climate.~~

We bias correct the downscaled model temperatures ~~and precipitation~~ output by using ~~Berkeley~~CRU gridded ~~temperature data and GPCC gridded precipitation~~ data as a reference climate. Downscaled series were produced for each climate model for the period 2013 to 2089 under each climate scenario by averaged monthly differences over the baseline period 1980 to 2005 taken from the ~~models'~~ CMIP5 *historical* simulations ~~of the models~~. We only use summer (JJA) mean near-surface air temperature. Therefore, future temperature time series  ~~$T_i(t)$~~   $T_i(t)$  on each grid ~~point~~ were calculated by

$$\cancel{T_i(t)} = \cancel{T_{i,c}(t)} + (\cancel{\bar{T}_{i,Berkeley}} - \cancel{\bar{T}_{i,c,history}}), \quad i = 6, 7, 8.$$

$$T_i(t) = T_{i,c}(t) + (\bar{T}_{i,CRU} - \bar{T}_{i,c,history}), \quad i = 6, 7, 8 \quad (7)$$

where  ~~$T_{i,c}(t)$~~   $T_{i,c}(t)$  is monthly mean temperature for the  $i$ th month from the climate model output from  $t = 2013$  to  $2089$ ,  ~~$\bar{T}_{i,Berkeley}$~~   $\bar{T}_{i,CRU}$  and  ~~$\bar{T}_{i,c,history}$~~   $\bar{T}_{i,c,history}$  are mean temperature from ~~Berkeley Earth project~~CRU TS V 3.24 dataset and climate model output, respectively, for the  $i$ th month averaged over the baseline period 1980-2005 on each grid ~~point~~.

## 4. Results

### 4.1 Regional temperature and Future precipitation ~~change~~time series ~~$P_i(t)$~~ on each grid point were calculated by

~~Using the downscaled climate data (section 3), we estimate the mean surface air~~

temperature and precipitation anomalies during 2030–2069 simulated by the relevant model ensembles under G3, G4, RCP4.5 and RCP8.5 (Fig. 2 and Fig. 3). Over the period from 2030 to 2069, the regional average temperature increases moderately by  $0.17 \pm 0.18$  °C under G3 compared with the baseline (taken as the ensemble mean of each model’s RCP4.5 average over 2010–2029; Table 3). The temperature increases mainly over the north of the study region (including Tien Shan and Pamir). The regional average over 2030–2069 increases by  $0.50 \pm 0.34$  °C under G4, and  $1.30 \pm 0.34$  °C under RCP4.5 compared with the baseline. The ensemble mean temperature under G4 tends to decrease over the Himalayas, but with low model agreement.

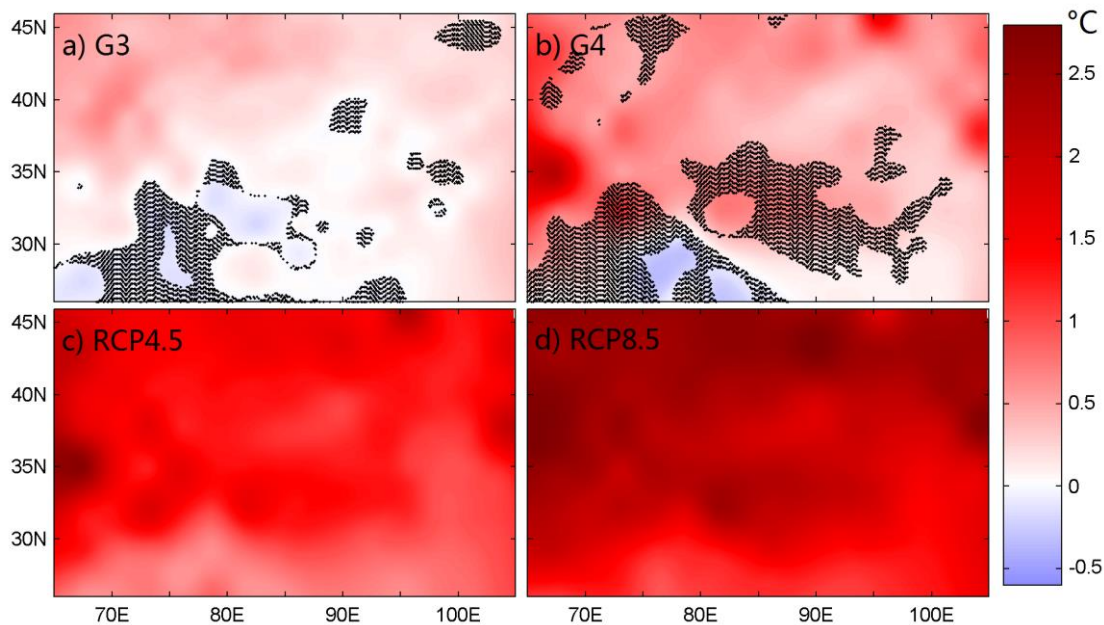


Fig 2. Ensemble mean surface air temperature anomalies during 2030–2069 simulated under G3 (a); G4 (b); RCP4.5 (c); RCP8.5 (d). The ensemble members are listed in Table 2. Anomalies are relative to the baseline RCP4.5 climate state between 2010 and 2029. Stippling indicates where fewer than 2/3 models agreed on the sign of change for (a), fewer than 4/5 models agreed for (b), fewer than 5/6 models agreed for (c) and (d).

Regional averaged precipitation under G4 and RCP4.5 between 2030 and 2069 are increased by  $0.05 \pm 0.08$  mm day<sup>-1</sup> and  $0.07 \pm 0.10$  mm day<sup>-1</sup>, respectively, compared with the baseline and slightly more for RCP8.5 (Table 3). The precipitation under G4 increases over most of the area but with low model agreement. The patterns of

precipitation change under G4 are similar to those under RCP4.5 and RCP8.5. The precipitation anomaly value increases from west to east and reaches the maximum in the south east of the region. The ensemble mean of the regional average precipitation change under G3 is negligible relative to the baseline, and the across-model variation is much larger than the ensemble mean. The precipitation change ratios under the 3 climate scenarios are from -15% to 10% (Fig. 3).

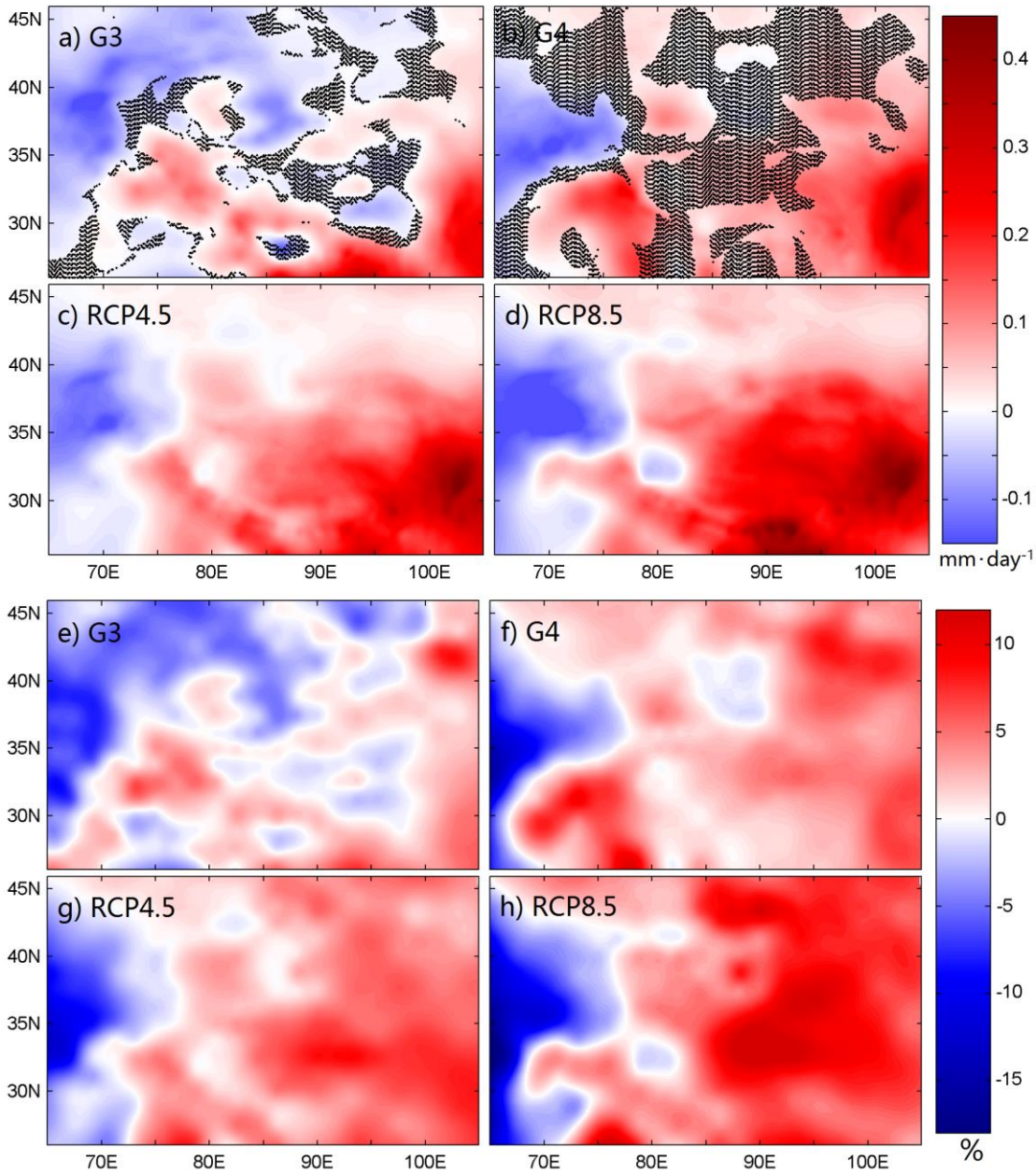


Fig. 3. As that for Fig. 2 but for precipitation anomalies (a-d) and precipitation percentage change (e-h).

#### 4.2 Temperature forcing for glacier change

The across-region summer mean temperature projections ensembles under G3, G4, RCP4.5 and RCP8.5 are shown in Fig. 4. We use Berkeley gridded temperature before 2013 and ensemble means of climate models (Table 2) with model bias correction (Section 3.2) under RCP4.5 from 2014 to 2019, and that under climate scenarios G3, G4, RCP4.5 and RCP8.5 from the year 2020 to 2089. We ensure that means of all ensembles at each grid point are equal at the year 2020. Figure 5 shows the time series of JJA mean temperature forcing from the beginning years to 2089. The temperature averages over the whole region and glaciated parts have similar trends.

Temperatures under RCP8.5 increase linearly and the highest rate among all the scenarios. Temperature increases under RCP4.5 are next, and its rate becomes smaller after about the year 2050 as specified greenhouse gas emissions decline. There is an obvious cooling effect (about  $0.75^{\circ}\text{C}$ ) projected by G4 compared with RCP4.5 during 2020–2069 over the whole region (Fig. 5). There is no trend in temperature under G3 in the geoengineering period (2020–2069). But after the termination in the year 2069, there is a temperature rise of about  $1.7^{\circ}\text{C}$  under G3. There is no similar termination rise under G4 where the temperature trend in the post-geoengineering period is almost the same as that earlier.

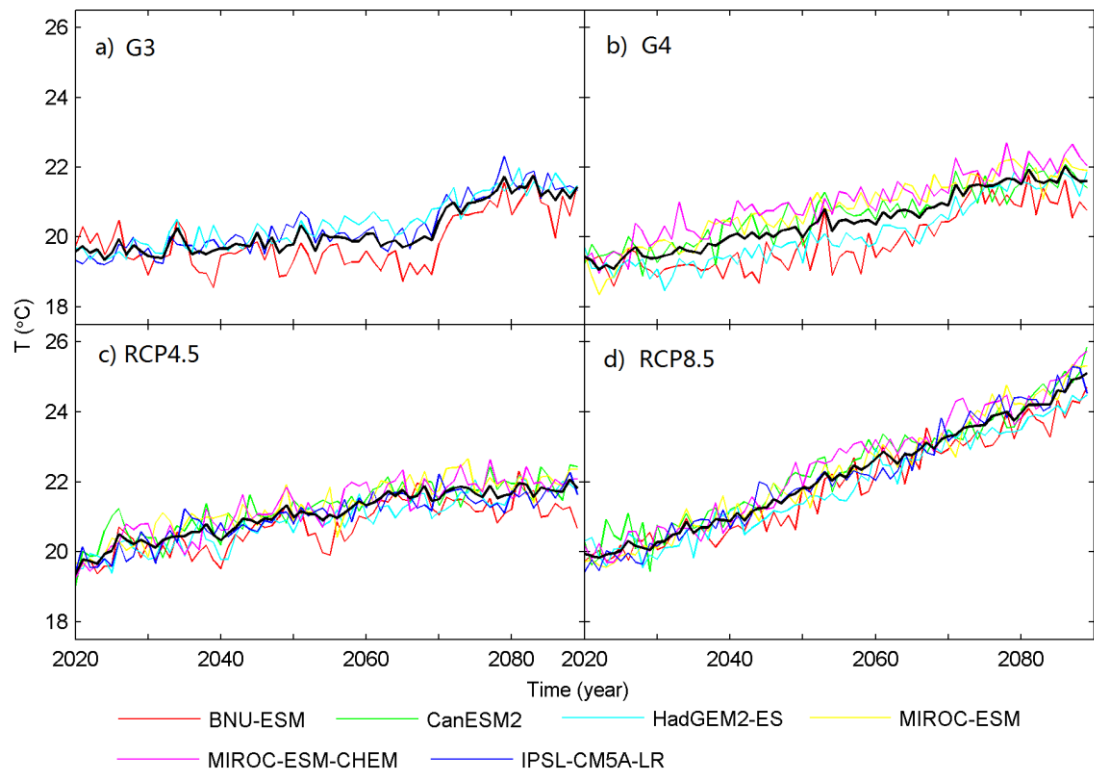


Fig. 4. Time series of summer mean temperature averaged over the grids in the whole region projected by ensemble members after model bias correction under climate scenarios G3 (a), G4 (b), RCP4.5 (c) and RCP8.5 (d). Black curve in each plot is the mean of the ensemble.

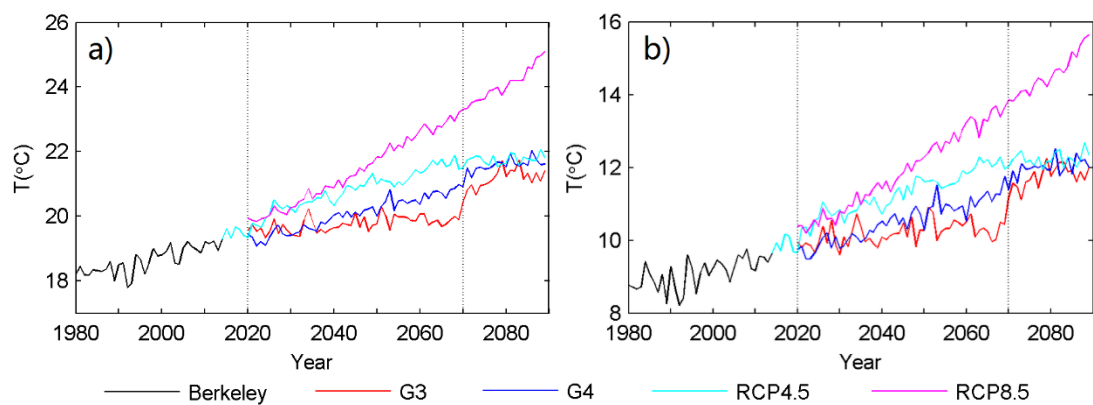
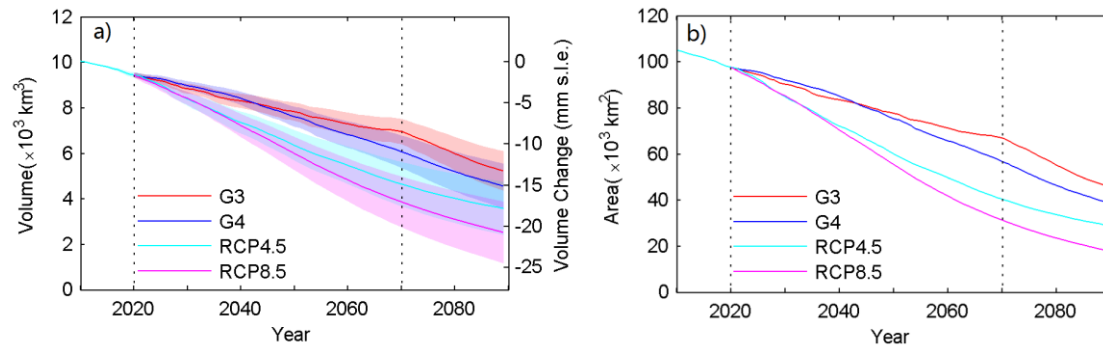


Fig. 5. Time series of summer mean temperature averaged over the grids in the whole region (a) and only in the glaciated region (b). Note the different temperature ranges.





**Fig. 6.** Total glacier volume in HMA (a) and the equivalent sea level rise assuming an ice density of  $900 \text{ kg m}^{-3}$  and ocean area of  $362 \times 10^{12} \text{ m}^2$  and (b) area changes from 2010 to 2089. Uncertainty in a) reflects factors in the statistical model discussed in section 4.3.

### 4.3 Glacier change

#### 4.3.1 Under different climate forcing

Glacier volume changes for all the glaciers in the study region computed using temperature data from the four scenarios are shown in Fig. 6a. Volume loss rates increase from G3, G4, RCP4.5 to RCP8.5 for the period 2020–2089. The RCP4.5 and RCP8.5 scenarios produce similar continuous mass loss until approximately 2035, and both show relatively slower loss rates after about the year 2050. The glacier volume loss in equivalent to sea level rise for the whole study region from 2010 to the end of geoengineering in 2069 is 8.4 mm (G3), 10.7 mm (G4), 14.7 mm (RCP 4.5) and 16.8 mm (RCP8.5), with 93.3%, 95.7%, 99.4% and 100% glaciers retreating under these scenarios. Therefore, the geoengineering schemes G3 and G4 help to reduce glacier mass loss in our simulations, and G3 reduces glacier loss more than G4.

There is a clear increase in volume loss rate under G3 after 2069 when geoengineering is terminated. Comparing the last 15 years of geoengineering (2055–2069) with the first 15 years of post-geoengineering (2070–2084) shows annual mean volume loss rate for all the glaciers of  $0.39\% \text{ a}^{-1}$  (referenced to the volume in the year 2010) increases to  $0.90\% \text{ a}^{-1}$ , which is higher than the rates of  $0.56\% \text{ a}^{-1}$  for RCP4.5 and  $0.70\% \text{ a}^{-1}$  for RCP8.5. However, the volume loss rate under G4 shows negligible termination effect; annual mean volume loss rates change from  $0.73\% \text{ a}^{-1}$  to  $0.78\% \text{ a}^{-1}$ .



before and after the termination. The glacier volume loss over the post geoengineering period of 2070–2089 for both G3 (4.8 mm) and G4 (4.1 mm) are higher than for either RCP 4.5 (3.0 mm) or RCP8.5 (3.7 mm). However, by 2070 under both RCP scenarios there is much less glacier ice volume remaining than under G4, or especially G3. Comparing ice loss rates at comparable total volumes, loss rates with RCP8.5 are similar to those of post geoengineering G3.

Glacier area change trends under each climate scenario are quite similar to the volume change trends (Fig. 6b). We project 44%, 37%, 28% and 17% of the area in 2010 remaining in the year 2089 under the G3, G4, RCP 4.5 and RCP8.5 scenarios, respectively.

#### 4.3.2 Variations across sub-regions

Glacier volume changes in the HMA sub-regions are shown in Fig. 7. Glacier volumes in most sub-regions decrease for the whole period, with the highest rates under RCP8.5 and lowest under G3, as expected. Glacier volume in inner Tibet under G3, and in eastern Himalaya under both G3 and G4 are unchanging or slightly increasing in the geoengineering period 2020–2069, because the summer mean air temperature has no trend there. The “termination effect” of geoengineering under G3 is significant in most sub-regions. However, there is no obvious change in glacier volume loss rate before and after 2070 under G4.

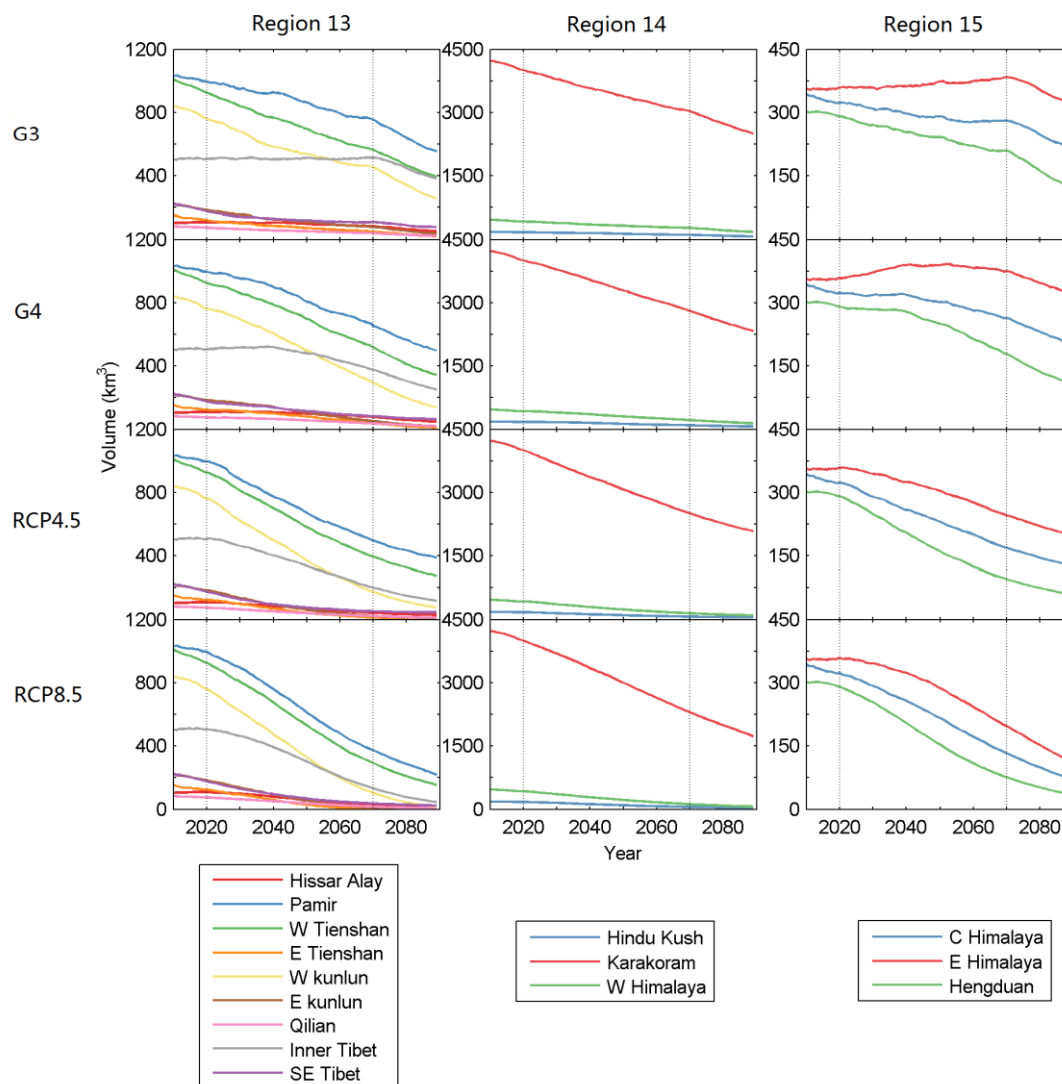


Fig. 7. Glacier volume (unit: km<sup>3</sup>) change from 2010 to 2089 for glaciers in sub-regions of Region 13 (left column), 14 (middle column) and 15 (right column) under scenarios by row from G3 (top), G4, RCP4.5, to RCP8.5 (bottom). The curves for sub-regions are colour-coded in the legend.—

#### 4.4 Uncertainties in projections—

There are several uncertainties in this study. Firstly, there only 3 ESMs participated in G3 than in G4 simply because doing the G3 experiment is difficult and time-consuming to set-up. So the ensemble climate projection is less robust in G3 than in G4. Secondly, although the goal of geoengineering schemes is to mitigate temperature warming, it inevitably also alters other important climate parameters, such as precipitation. We do not consider the impact of precipitation change on glacier change in this study, as the

climate models do not simulate significant precipitation changes in the HMA region (Table 3). However, there will be generally less precipitation under geoengineering scenarios that balance long wave greenhouse gas radiative forcing with short wave forcing than under the RCP4.5 or RCP8.5 scenarios (Tilmes et al., 2013), which would be expected to lead to increased ice loss. So potentially our estimates of glacier wastage under G3 and G4 scenarios may be under-estimated. Simulating change in the Asian monsoon is difficult for climate models under geoengineering since the deep convention involved may also be influenced by chemistry changes in the stratosphere caused by the injected aerosols—most of the ESM models in our study do not have sophisticated aerosol chemistry schemes (though the MIROC ESM-CHEM model does). Thirdly, we note that the distribution of meteorological stations in the study region is very sparse, especially in the northwest of this region (Liu and Chen, 2000).

Therefore, both the Berkeley gridded data and temperature data from models projections that we used in this study may have low accuracy for specific glacier regions. There are several key parameters in our algorithm which influence the modeled

$$P_i(t) = P_{i,c}(t) \cdot \frac{\bar{P}_{i,GPCC}}{\bar{P}_{i,c,history}}, \quad i = 1, \dots, 12 \quad (8)$$

where  $P_{i,c}(t)$  is monthly precipitation for the  $i$ th month from the climate model output from  $t = 2013$  to  $2089$ ,  $\bar{P}_{i,GPCC}$  and  $\bar{P}_{i,c,history}$  are monthly precipitation from GPCC dataset and climate model output, respectively, for the  $i$ th month averaged over the baseline period 1980-2005 on each grid point.

The temperature and precipitation on each glacier were calculated by an altitude temperature lapse rate of  $0.65^\circ\text{C}/100\text{ m}$ , precipitation lapse rate of  $3\%/100\text{ m}$ , and the elevation difference of the glacier surface elevation relative to the nearest fine grid point. Moreover, the solid precipitation on the glacier is calculated by the fraction of solid precipitation,  $f_{solid}$ , based on the monthly mean temperature  $T_a$  on the glacier as (Fujita and Nuimura, 2011)

$$f_{solid} = \begin{cases} 1, & \text{if } T_a \leq 0^\circ\text{C} \\ 1 - \frac{T_a}{4}, & \text{if } 0 < T_a < 4^\circ\text{C} \\ 0, & \text{if } T_a \geq 4^\circ\text{C} \end{cases} \quad (9)$$

### 3.3 Validation of the glacier volume loss model and were summarized methodology

In this section we justify the selection of various parameter values used in the method here. In section 5 we indicate how elements in the model and climate forcing affect the uncertainties of the results we produce in section 4, and how those results compare with previous estimates of glacier evolution in HMA.

A crucial parameterization concerns the SMB-altitude gradients. The field data (Table 1) include three more glaciers than those used in Zhao et al. (2014; 2016). Here, and include a benchmark glacier from almost every sub-region. With so few glacier observations available, there is an issue of how representative they are of the general population. For inner Tibet, there are three glaciers (Zhadang, Gurenhekou and Xiao Dongkemadi Glacier) with SMB observations, and they have almost the same SMB-altitude gradients,  $0.0041 \text{ m m}^{-1}$ , over their common elevation range (5515~5750 m, Table 1); two glaciers (Naimona'nyi and Kangwure) in central Himalaya have SMB gradients of  $0.0038 \text{ m m}^{-1}$  in their common altitude range of 5700~6100 m. These similarities suggest that the measured glaciers share some important characteristics with the vast majority which are not surveyed.

Next we consider the uncertainty resulting from using different choices for the initial value of ELA at the start year, different V-A scaling parameters and the effect of different ELA sensitivities to summer mean temperature and annual precipitation.

For choosing the initial ELAs for each glacier, there are several alternative choices are reasonable: we can use the ELA alternatives (Zhao et al., 2016): i) using ELAs interpolated from the first Chinese glacier inventory, or ii) median elevations from RGI dataset, or iii) the elevation of the 60th percentile of the cumulative area above the glacier terminus (Zhao et al., 2016). These three choices lead to a range with coefficient of variation about 2.5 mm of 13% global sea level in glacier volume loss at 2050. In this

study, we use median elevations from RGI dataset, which corresponds to the median result.

Including an ELA precipitation sensitivity prescribed from Rupper and Roe (2008) and annual precipitation change rates over the period 1980–2050 from a high resolution regional model RegCM3 (Gao et al., 2012) forced by the IPCC A1B greenhouse gas scenario leads to a reduced glacier loss of about 12% (Zhao et al., 2016) compared with rates when driven by temperature forcing alone. This is because most greenhouse gas forcing scenarios produce slight increases in precipitation over the HMA (Fig. 3). Here we do not take ELA sensitivity to precipitation into account and Table 3 suggests no reason to expect significant changes in precipitation across the region under either geoengineering or RCP scenarios.

Analysis by Zhao et al. (2014) showed that different volume-area scaling parameterizations can lead to  $\pm 5\%$  range of glacier volume loss. The set of parameters we use in this study corresponds to the lower bound of estimated volume loss, but one that is best matched to the observational data. Combining dataset of 230 separate glaciers (Moore et al., 2013).

For the ELA sensitivity to summer mean temperature and annual precipitation, we use the zonal mean values from energy-balance modelling of glaciers in HMA by Rupper and Roe (2008). Alternatively, it can be estimated using an empirical formula for ablation and a degree-day method (Zhao et al., 2016). Zhao et al. (2016) calculated the ELA for nine glaciers in China, India and Kyrgyzstan, and compared them with the observed ELA time series by similarities of decadal trends and also annual variability. The Rupper and Roe ELA parameterization produced the best fits to observed ELA decadal trends on 9 glaciers, with a correlation coefficient of 0.6 which is significant ( $p < 0.05$ , the values we give for  $p$  are single tailed Pearson correlation tests).

Combining the above ~~three~~ uncertainties would require a Monte Carlo simulation since the parameters combine non-linearly to produce glacier volume and area change; this is prohibitively expensive to perform given that a single simulation of all glaciers in HMA requires about 60 cpu hours on an 8 ~~core computer with parallel computing in~~ Matlab. We can illustrate the uncertainty range by assuming parameter errors are

~~independent and ignore inherent non-linearity, which leads to an uncertainty range of about  $\pm 18\%$  in glacier volume losses (Fig. 6).~~ cores computer with parallel computing in Matlab. We did estimate elevation changes for individual glaciers directly from simulated volume and area changes, then calculated the average rate of elevation change for all the glaciers in each sub-region and compared them with remote-sensing estimates from 2003 to 2009 from Gardner and others (2013), Table 2. The correlation coefficient between the Gardner et al. (2013) estimates for the 6 RGI 5.0 sub-regions with data regional and our modeled regional averages is 0.7 which is marginally significant, ( $p < 0.1$ ).

~~One further key parameter is the ELA sensitivity to summer mean temperature. Here we use the zonal mean values from energy balance modelling of glaciers in HMA by Rupper. In our simulations we have used constant lapse rates for temperature ( $0.65^\circ\text{C}/100\text{ m}$ ) and Roe (2008). Alternatively, it can be estimated using an empirical formula for ablation and a degree-day method (Zhao et al., 2016). However, precipitation (3%/100 m). To check how reliable this is we prefer the Rupper chose 5 meteorological stations close to glaciers and calculated correlation coefficients for JJA temperature and Roe annual precipitation at the station and at the nearest downscaled grid point from 1980 to 2013 ( $n=34$ ). Precipitation correlations were higher than 0.85 for all the stations ( $p < 0.001$ ), while temperatures correlations were 0.47-0.85 ( $p < 0.01$ ).~~

~~Finally we explored the sensitivity to the choice of dataset used to correct model estimates since the bias in temperatures. In addition to using historical temperature from the CRU dataset, we also did the simulation using temperature from Berkeley Earth project ( $1^\circ \times 1^\circ$  resolution; Rohde et al., 2013; <http://berkeleyearth.org/data/>). That simulation was done using temperature alone as the glacier driver, so precipitation for each glacier was constant over time. The simulated variation climate ensemble mean forced volume losses in ELA over time the period 2010-2069 were +4% (G3), -9% (G4), -11% (RCP4.5) and -13% (RCP8.5) different from the results using the CRU dataset.~~

## 5. Results

### 4.1 Climate and glacier change across HMA



---

#### **4.1.1 Temperature and precipitation over HMA**

We construct the climate forcing by using CRU temperature ~~fit best~~ data and GPCC precipitation data before 2013 and climate models (Table 3) with ~~observed~~ model bias correction (Section 3.2) under RCP4.5 from 2014 to 2019, and that under climate scenarios G3, G4, RCP4.5 and RCP8.5 from the year 2020 to 2089. The JJA mean temperature projections in the whole region under G3, G4, RCP4.5 and RCP8.5 from 2020 to 2089 are shown in Fig. 2. Figure 3 shows the time series of ~~ELA-decadal~~ JJA mean temperature and annual precipitation forcing from the beginning years to 2089, with the across-model range from the ensemble members; ranges found are slightly smaller than the regional spread found by Yu et al. (2015) due to grid-point by grid-point bias correction we apply here.

The multi-model mean temperature under G4 is higher than that under G3 in the geoengineering period. In contrast with the ensemble mean temperature, the HMA mean temperature projected by HadGEM2-ES under G4 is cooler than that under G3; and its G4 temperature is lower than the ensemble mean while its G3 is higher than the ensemble mean (Fig. 2). The across-model spread in temperature response to G4 is larger than that under G3. Temperatures projected by BNU-ESM are lower than ensemble mean under both G3 and G4.

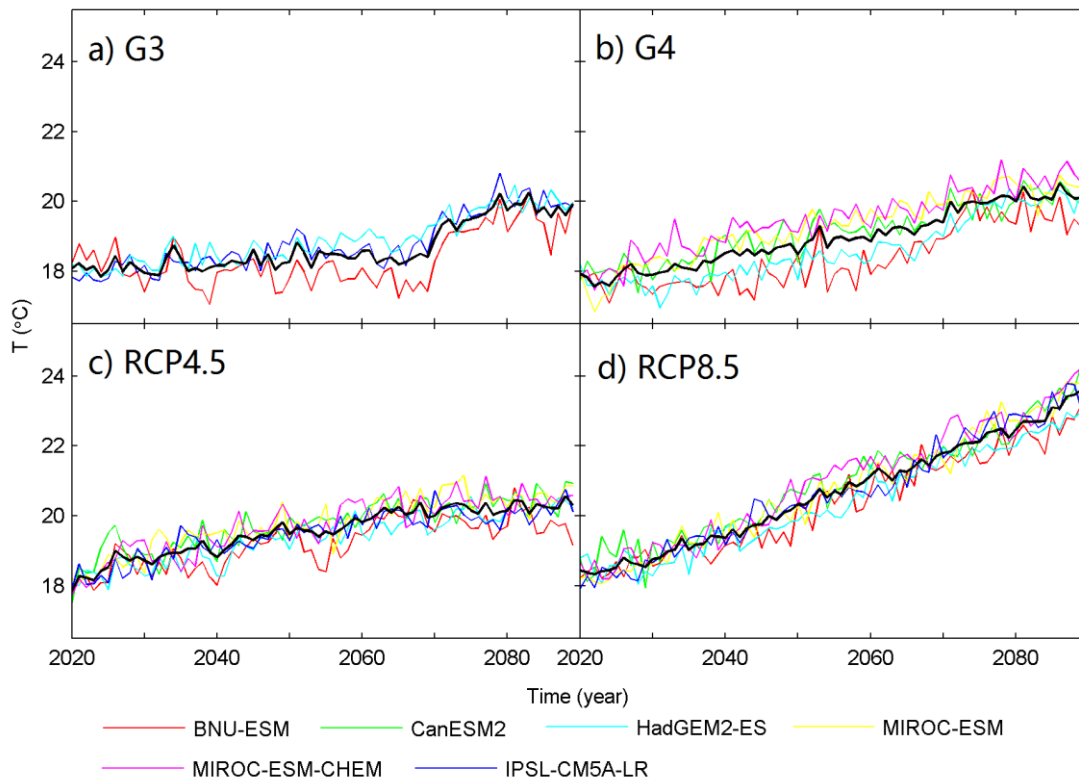


Fig. 2. Time series of summer mean temperature averaged over the downscaled grid in the whole HMA region projected by ensemble members after model bias correction under climate scenarios G3 (a), G4 (b), RCP4.5 (c) and RCP8.5 (d). Black curve in each plot is the mean of the relevant ensemble (Table 3).

The temperature averages over the whole region and the glaciated parts have similar trends on nine. Temperatures under RCP8.5, as expected, increase at the highest linear rate among all the scenarios. Temperature rises under RCP4.5 are next highest, and its rate becomes smaller after about the year 2050 as specified greenhouse gas emissions decline. There are relative coolings of 1.05° C under G3 and 0.76° C under G4 compared with RCP4.5 during 2020-2069 across the whole region (Fig. 3). Yu et al. (2015) noted that G3 produced a relative cooling under G3 of 0.58° C and G4 of 0.53° C in globally averaged temperature over the 2030-2069 period.

There is no trend in temperature under G3 over the geoengineering period (2020-2069). But after the termination in the year 2069, there is a temperature rise of about 1.3° C over the period 2070-2089 relative to the period 2050-2069 under G3. There is

a less obvious termination rise of temperature under G4 than that under G3. This is due to G4 having a constant stratospheric aerosol injection rate of 5 Tg SO<sub>2</sub> per year, while G3 gradual ramps-up the aerosol so that about twice as much is needed by 2069, depending upon the sensitivity of the particular model to stratospheric sulphate aerosols. Hence, the radiative impact of terminating G3 is about twice as large as terminating G4, and the termination temperature signal is much more obvious in G3 than G4.

The annual precipitation averages over the whole region do not show obvious trends in any climate scenarios (Fig. 3c). However, the annual solid precipitation averages over the glaciers show decreasing trends in all the scenarios (Fig. 3d) until 2070, which is due to increases in surface air temperature (Fig. 3b). Under RCP8.5, annual solid precipitation averaged over each glacier decreases fastest (2.2 mm a<sup>-1</sup>). Decreases are similar (about 1.5 mm a<sup>-1</sup>) under RCP4.5 and G4 and least (0.3 mm a<sup>-1</sup>) under G3 during the geoengineering period (2020-2069). After the year 2070, there are no trends in annual solid precipitation under G3, G4 and RCP4.5 (Fig. 3d) due to stable temperatures (Fig. 3b).

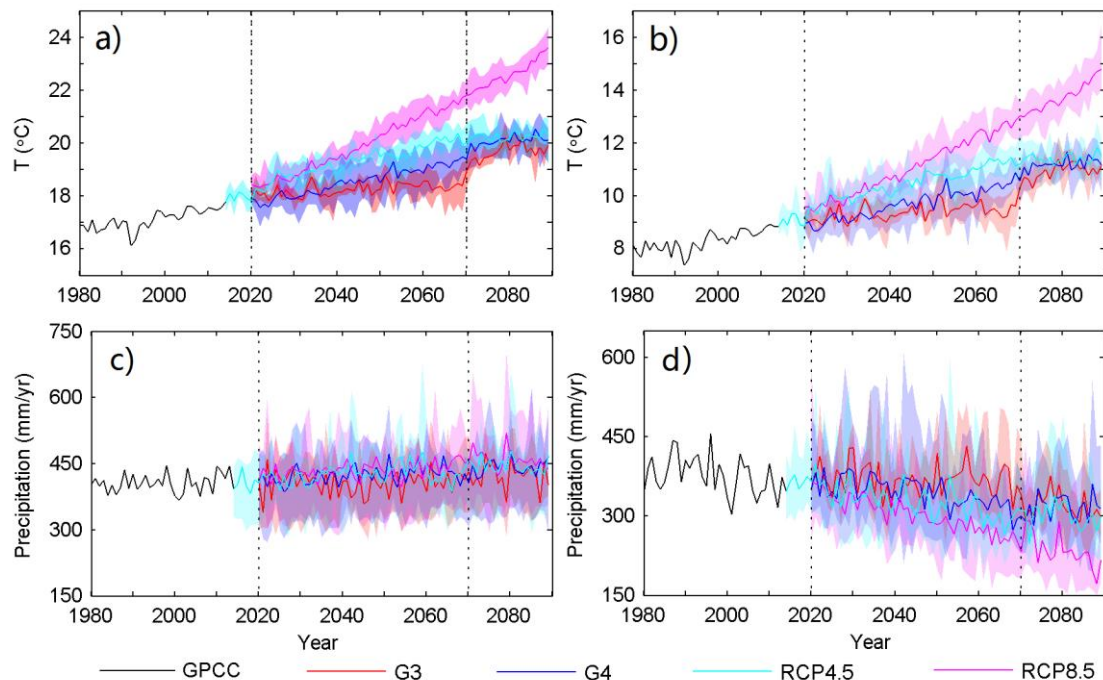


**Fig. 3.** Time series of summer mean temperature (a, b) and annual precipitation (c, d) averaged over the downscaled grid (section 3.2) in the whole region (a, c) and only in the glaciated region (b, d). Note the different temperature ranges in plot (a) and plot (b)

and precipitation ranges in plot (c) and plot (d). Precipitation in plot (d) is the average annual solid precipitation at the ELA of each glacier in the start year of simulations which is taken here to be representative of each glacier. The solid curves and shadings from 2013 to 2089 are ensemble mean and the across-model spread between ensemble members for each scenario, which are colour-coded in the legend.

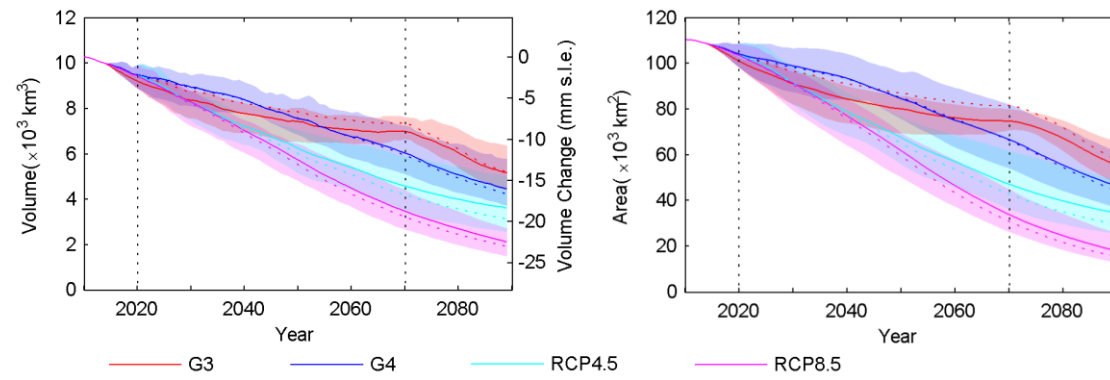


**Fig. 4.** Total glacier volume in HMA (a) and the equivalent sea level rise assuming an ice density of  $900 \text{ kg m}^{-3}$  and ocean area of  $362 \times 10^{12} \text{ m}^2$  and area (b) from 2010 to 2089. The solid curves and shadings are means of individual climate model forced simulations and the across-model spread, for colour-coded scenarios. The dashed curves are results using multi-model ensemble mean temperature and precipitation forcing under each scenario.

#### 4.1.2 Glacier changes across HMA

Glacier volume changes for all the glaciers in the study region computed using temperature and precipitation data from the four scenarios are shown in Fig. 4a. The uncertainty we plot is due only to the differences between climate forcing across the models, it does not reflect uncertainty of the glacier model parameters. Volume loss rates increase from G3, G4, RCP4.5 to RCP8.5 for the period 2020-2069. The RCP4.5 and RCP8.5 scenarios produce similar continuous mass loss until approximately 2035 (Fig. 4a) mainly due to the similarity of temperatures projected by RCP4.5 and RCP8.5 in the period 2020-2035 (Fig. 3a), and both show relatively slower loss rates after about the year 2050 probably because the most sensitive glaciers have already retreated before

2050. Volume loss using the climate projected by HadGEM2-ES under G4 is far less than that by other models (Table 4), so we exclude it when calculating the G4 model mean. The multi-model mean glacier volume loss is equivalent to sea-level rise for the whole study region from 2010 to the end of geoengineering in 2069 is 9.0 mm (G3), 11.7 mm (G4), 15.5mm (RCP 4.5) and 18.5 mm (RCP8.5), with 91.8%, 96.0%, 98.5% and 99.7% glaciers retreating under these scenarios (Table 4). These numbers may also be compared with the simulations run using the ensemble mean climate forcing (last row in Table 4), which are all close to the means of the individual model driven mass losses, as are the time varying loss rates (Fig. 4). This is despite the mean climate ensemble including the HadGEM2-ES results for G4. Therefore, the geoengineering schemes G3 and G4 help to reduce glacier mass loss in our simulations, and G3 reduces glacier loss more than G4, which is due to stronger temperature cooling effect under G3 (section 4.1.1).

There is a clear increase in volume loss rate under G3 after 2069 when geoengineering is terminated. Comparing the last 15 years of geoengineering (2055-2069) with the first 15 years of post-geoengineering (2070-2084) shows annual mean volume loss rate for all the glaciers of  $0.17\% \text{ a}^{-1}$  (referenced to the volume in the year 2010) increases to  $1.11\% \text{ a}^{-1}$ , which is higher than the rates of  $0.54\% \text{ a}^{-1}$  for RCP4.5 and  $0.66\% \text{ a}^{-1}$  for RCP8.5. However, the volume loss rate under G4 shows negligible termination effect; annual mean volume loss rates change from  $0.73\% \text{ a}^{-1}$  to  $0.86\% \text{ a}^{-1}$  before and after the termination. The glacier volume loss over the post geoengineering period of 2070-2089 for both G3 and G4 are higher than for either RCP 4.5 or RCP8.5 (Table 4). However, by 2070 under both RCP scenarios there is much less glacier ice volume remaining than under G4, or especially G3. Comparing ice loss rates at comparable total volumes, loss rates with RCP8.5 are similar to those of post geoengineering G3.

As may be expected, glacier area change trends under each climate scenario are similar to the volume change trends (Fig.4b). We project 53%, 41%, 27% and 14% of the area in 2010 remaining in the year 2089 under the G3, G4, RCP 4.5 and RCP8.5 scenarios, respectively.

---

## **4.2 Sub-regional climate and glacier changes**

### **4.2.1 Sub-regional temperature and precipitation change**

There are three RGI 5.0 regions in HMA: Central Asia, South Asia West and South Asia East. They are named as Region 13, 14 and 15 and sub-divided into smaller sub-regions in the RGI 5.0 dataset (Fig. 1). In this section we plot the averages of JJA-mean temperatures (Fig. 5) and that of annual solid precipitation at the ELA of every glacier in the start year (Fig. 6) in every sub-region under all the climate scenarios.

Temperatures under RCP8.5 increase at the highest rates ( $0.053\sim0.087^{\circ}\text{C a}^{-1}$ ) among all the scenarios, with temperature increases under RCP4.5 in the range of  $0.030\sim0.059^{\circ}\text{C a}^{-1}$  with its rate decreasing after about the year 2050 as specified greenhouse gas emissions decline. The temperatures rises of  $0.030\sim0.050^{\circ}\text{C a}^{-1}$  occur under G4 across the sub-regions. Under RCP4.5, RCP8.5 and G4, temperatures increase slowest in the southeast of the study area (S and E Tibet, C Himalaya, E Himalaya and Hengduan Shan) and fastest in the northwest (mainly Tien Shan, Hissar Alay, Karakoram, Pamir, and Hindu Kush).

There is no trend in temperature under G3 in the geoengineering period (2020-2069) in all the sub-regions. The temperature cooling projected by G3 compared with RCP4.5 during 2020-2069 is about  $1.0^{\circ}\text{C}$  in sub-regions of Central Asia,  $1.2^{\circ}\text{C}$  in South Asia West, and  $0.8^{\circ}\text{C}$  in South Asia East (Fig. 5). After the termination in the year 2069, there are temperature rises of about  $1.07\sim1.65^{\circ}\text{C}$  over the period 2070-2089 relative to the period 2050-2069 under G3. The post-termination temperatures increase least (about  $0.020^{\circ}\text{C a}^{-1}$ ) in Karakoram and the most (about  $0.046^{\circ}\text{C a}^{-1}$ ) in Eastern Kunlun. The temperature cooling projected by G4 compared with RCP4.5 during 2020-2069 is very similar across all the sub-regions,  $0.68\sim0.86^{\circ}\text{C}$ .



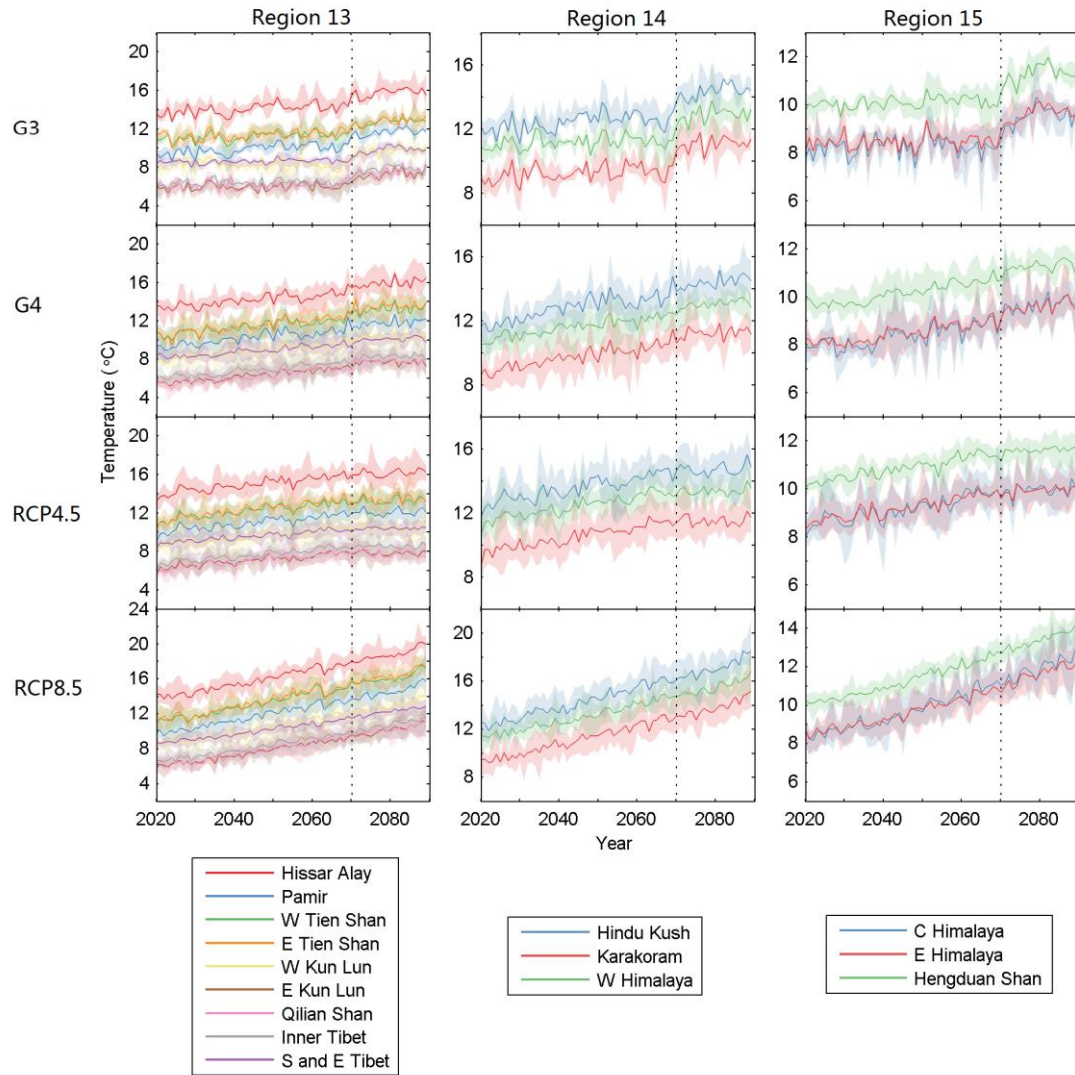


**Fig. 5. JJA-mean surface air temperature time series from 2010 to 2089 in the sub-regions of Region 13 (left column), 14 (middle column) and 15 (right column) under scenarios by row from G3 (top), G4, RCP4.5, to RCP8.5 (bottom). Note the different temperature ranges in the panels. The curves and shadings are ensemble mean and the spread between ensemble members for sub-regions, which are colour-coded in the legend.**

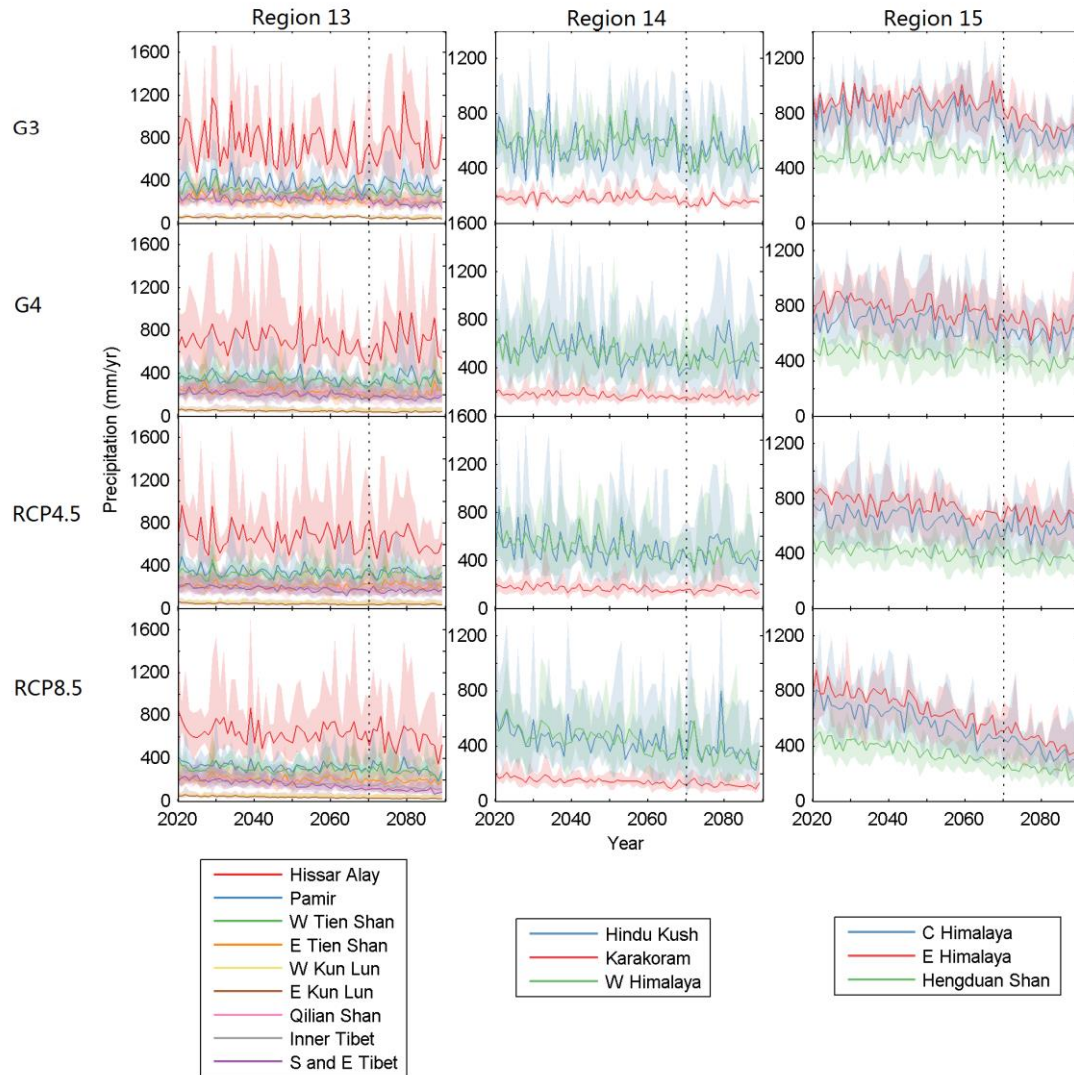


Fig. 6. As that for Fig. 5 but for annual solid precipitation on the glacier.

The annual solid precipitation projected by RCP8.5, and to a lesser degree by RCP4.5 and G4, decreases in all the sub-regions, with the rates larger than  $1.5 \text{ mm a}^{-1}$  in S and E Tibet, Hindu Kush, W Himalaya and the whole of Region 15 (C Himalaya, E Himalaya, Hengduan). There is no obvious trend of solid precipitation projected by G3 in the geoengineering period (2020-2069) in most sub-regions. But after the geoengineering termination under G3 in the year 2069, there is a significant decrease of solid precipitation in S and E Tibet, Hindu Kush, and the whole of Region 15.

#### 4.2.2 Sub-regional glacier changes

Glacier volume changes in the HMA sub-regions are shown in Fig. 7. Glacier volumes in all the sub-regions decrease during the period 2020-2089, with the highest rates under

RCP8.5 and the second high rates under RCP4.5, as expected. Glacier volumes decrease with lower rates under G3 and G4 in all the sub-regions except S and E Tibet, inner Tibet, and Hengduan Shan, where glacier volumes increase from the year 2020 to about 2040 under G4, and to the end of geoengineering period under G3 (Fig. 7). The glacier volume triples in S and E Tibet and increases by about 56% in inner Tibet, while increasing slightly in Hengduan Shan in the geoengineering period under G3. The “termination effect” of geoengineering under G3 is significant in most sub-regions.

There are some noticeable difference between means of individual climate model forced simulations and the results using multi-model ensemble mean climate forcing. (Fig. 7). For example, S and E Tibet under all the scenarios, Karakoram under G3, and inner Tibet under G4. This could be because i) individual model differences in temperature and precipitation forcings are large between ensemble members and their means (especially for the 3 model ensemble in G3) in particular sub-regions; ii) glacier hypsometry differences between regions lead to sensitivity under some combinations of forcing when the ELA change is located around large amounts of ice; iii) glacier data inside S and E Tibet was measured in 1970s (section 2) and contains outlines of glacier complexes rather than individual glaciers, which has an impact on the volume estimate because of the non-linearity of volume-area scaling relationship.

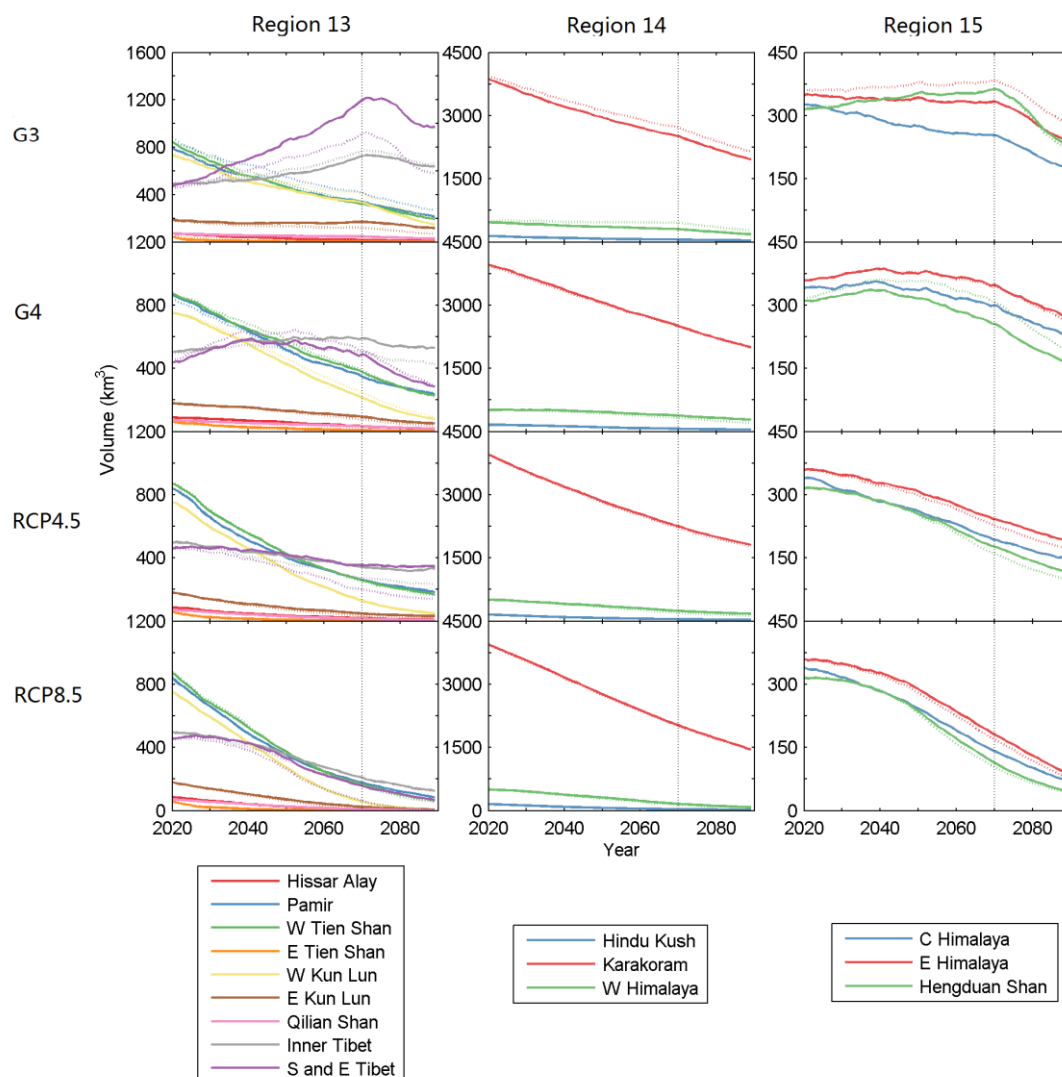


Fig. 7. As that for Fig. 5 but for glacier volume (unit:  $\text{km}^3$ ). The solid curves are means of individual climate model forced simulations. The dashed curves are results using multi-model ensemble mean temperature and precipitation forcing under each scenario. The across-model spread for each sub-region is not shown for clarity. Note the difference of glacier volume ranges in the panels.

## 5 Uncertainties in projections

Glacier model parameter selection was discussed in section 3.3, and in more depth by Zhao et al. (2016). In this section we address, and try to estimate, how systematic errors in climate forcing or glacier model parameters cause errors in projections of HMA glacier contributions of sea level rise.

### 5.1 Climate forcing

There are several uncertainties in climate model forcing used to drive the glacier model in this study. The models are also relatively coarsely gridded, certainly compared with the vast majority of glaciers, and so differences may be expected between statistically downscaled forcings based on lapse rates that we use here and that produced from high resolution dynamic climate model forcing.

Firstly, only 3 ESMs participated in G3 but 5 in G4 simply because doing the G3 experiment is difficult and time-consuming to set-up. So the ensemble climate projection by G3 is less robust than that by G4. In many cases it seems that the results from G3 and G4 are statistically similar enough to be combined (Yu et al., 2015, Moore et al., 2015). We tested the differences between RCP8.5, RCP4.5 and G4 using the 4 models in common (Table 4), and find the glacier responses are significantly different ( $p < 0.05$ ). Although there are too few models in common between G3 and G4, the dominant influence of summer melting to the mass balance across the region (Zhao et al., 2016), and the clear difference in temperature across HMA between G3 and G4 (Figs. 2,3) suggest the glacier response in HMA is different between G3 and G4.

Secondly, although the goal of geoengineering schemes is to mitigate temperature rises, it inevitably also alters other important climate parameters, such as precipitation. Simulating change in the Asian monsoon is difficult for climate models under geoengineering since the deep convection involved may also be influenced by chemistry changes in the stratosphere caused by the injected aerosols – most of the ESM models in our study do not have sophisticated aerosol chemistry schemes (though the MIROC-ESM-CHEM model does). Tilmes et al. (2013) showed that changes under the G1 scenario (which specified a much larger shortwave radiation reduction than G3 or G4), produced a weakening of the Asian monsoon and the hydrological cycle by about 5%. The reductions in solid precipitation (Fig. 3) under RCP8.5 are about 1/3 relative to historical levels, and the regions most affected in Region 15 (Fig. 6) are some of those most influenced by monsoon precipitation patterns (Fig. 1). Hence the temperature impact is probably more significant than changes in monsoon precipitation suggested by the G1 results discussed by Tilmes et al. (2013).

Thirdly, we note that the distribution of meteorological stations in the study region is

---

very sparse, especially in the northwest of this region (Liu and Chen, 2000).

## **5 Conclusion**

We Therefore, both the CRU gridded data and data from models projections that we used in this study may have low accuracy for specific glacier regions. This has also implications for the use of very high resolution dynamic models; one such model simulated air temperatures and down-welling radiative fluxes well, but not wind speed and precipitation, producing unstable results when used with the CLM45 land model that simulated ground temperatures and snow cover (Luo et al., 2013). Explicit glacier atmospheric mass balance modelling (Mölg et al., 2013), a technique based on very high spatial and temporal resolution climate data (hourly and 60 m) was used on Zhadang glacier (Fig. 1, Table 1) with in-situ observations available, but not across the general expanse of the glaciated region; this study also noted the importance of wind speed to glacier mass balance in the region influenced by the Indian monsoon. Maussion et al., (2013) demonstrate that 10 km resolution dynamic modelling of the region can be done successfully, and potentially can improve the precipitation modelling over the statistical downscaling methodology we employ here, though to date this is a reanalysis dataset with no prognostic simulations. Zhao et al. (2014 and 2016) used a 25 km resolution regional climate model RegCM3 to drive their simulations of glacier response to scenario A1B. By 2050 under A1B (which is intermediate between RCP4.5 and 8.5 in temperature rises), a sea level rise equivalent to 9.2 mm was projected from HMA. In comparison, our estimates are 11.1-12.5 mm for RCP4.5 and RCP8.5 (Fig. 4).

### **5.2 Glacier model**

The model we use is not particularly sophisticated, it simply relies on statistical relationships between mass balance and ELA. Compared with the method used in our previous study Zhao et al. (2014, 2016), we improved our method here by considering the area response time in the volume-area scaling (Eqn. (1)) which is more physical. We also allow the glacier area to grow (section 3.1), giving better estimates of glacier area for advancing glaciers. The motivation to use a relatively simple model must be that it simulates the glaciers well given the available data. As previously discussed there



is a shortage of observational data both on glaciers and from climate stations across HMA. In Section 3.3 we discussed how the model performs when tested against by the limited data available from satellites and ground measurements, in this section we compare the model against previous simulations of HMA glaciers under climate warming, and how its weaknesses may affect the reliability of projected mass changes.

Perhaps a strong limitation on the glacier simulation under geoengineering in our model is the lack of response to the changes in short wave forcing that would be produced under aerosol injection schemes. van de Berg et al. (2011) showed that Greenland mass balance during the Eemian interglacial could not be explained purely by temperature rises but must also include losses due to changes in the shortwave radiation flux on the ice sheet.

Testing our results for the greenhouse gas scenarios against previous studies; we project glacier volume loss, in equivalent sea-level rise, for all the glaciers from 2010 to 2089 as  $18.2 \pm 2.5$  mm and  $24.2 \pm 1.3$  mm under the RCP 4.5 and RCP8.5 scenarios, respectively. The volume change of all the glaciers in HMA over the 21th century estimated by Radić et al. (2014) is about  $15 \pm 5$  mm under RCP4.5 and  $22 \pm 5$  mm under RCP8.5. Marzeion et al. (2012) estimate about  $15.4 \pm 4.5$  mm under RCP4.5, and  $18.8 \pm 4.0$  mm under RCP8.5 using projected temperature and precipitation anomalies from ~~an~~ ensemble of 15 CMIP5 climate models. ~~These estimates are close to ours, despite their methodology being quite different from ours. The results projected by our method have higher means but smaller uncertainties than theirs, but do not differ significantly.~~

~~Terminating G3 geoengineering at 2069 leads to a rapid temperature rise and immediate increase in~~ The across-model uncertainties we plot here (Fig. 4) are smaller than glacier reduction, with method uncertainties (section 3.3; Zhao et al., 2016). Hence, more mass balance and meteorological stations on glaciers across the region, or longer and higher spatial resolution time series of glacier elevation changes, would better constrain the projected mass losses than simply increasing the number, or resolution, of climate models used in the simulations. That is the range of mass projections given by the mass balance model with different, but reasonable, choices of data-limited

quantities such as the ELA-sensitivity to temperature or the SMB-altitude gradients, is larger than the across model range for each climate scenario.

## 6 Summary and Conclusion

We estimate and compare glaciers volume loss ~~rates exceeding those for~~ glaciers in HMA using a statistical model based on glacier SMB parameterization to the year 2089. We construct temperature and precipitation forcing by using CRU temperature data and GPCC precipitation data before 2013, and projections from RCP86 Earth System Models running RCP4.5. ~~Furthermore even the most extreme~~ and RCP8.5 and the stratospheric sulphate aerosol injection geoengineering scenarios G3 and G4 with model bias correction and downscaling to a high resolution spatial grid based on fixed altitudinal lapse rates for temperature and precipitation. In assessing how glaciers respond to geoengineering ~~(G3) climates~~, we consider only across-climate model differences between the scenarios rather than uncertainties in glacier mass caused by errors in the glacier model we use. The projections suggest that glacier shrinkage at the end of the geoengineering period in 2069 are equivalent to sea-level rises of  $9.0 \pm 1.6$  mm (G3),  $11.5 \pm 2.5$  mm (G4 excluding HadGEM2-ES),  $15.5 \pm 2.3$  mm (RCP 4.5) and  $18.5 \pm 1.7$  mm (RCP8.5) relative to their volumes in 2010 (Table 4), with 91.8%, 96.0%, 98.5% and 99.7% glaciers retreating under these scenarios. There are clear increases in temperature and glacier volume loss rate under G3 after 2069 when geoengineering is terminated, which is higher than the rate under RCP8.5. But the termination effect under G4 is negligible. Glacier volumes decrease in most sub-regions under all the scenarios, while increase in inner Tibet, S and E Tibet and Hengduan Shan from the year 2020 to about 2040 under G4, and to the end of geoengineering period under G3.

Although G3 keeps the average temperature from increasing in the geoengineering period, G3 only slows glacier shrinkage by about 50% relative to losses from RCP8.5 ~~(8.4 and 16.8 mm sea level equivalent at 2069 respectively)~~. Approximately ~~65~~72% of glaciated area remains at 2069 under G3 compared with about ~~35~~30% for RCP8.5. The reason for the G3 losses is likely to be that the glaciers in HMA are not in equilibrium with present day climate, so simply stabilizing temperatures at early 21<sup>st</sup> century levels

does not preserve them. To do that would require significant cooling, perhaps back to early 20<sup>th</sup> century levels. Achieving that cooling by sulphate aerosol injection may not be possible. The 5 Tg of SO<sub>2</sub> per year specified in G4 is about the same loading as a 1991 Mount Pinatubo volcanic eruption every 4 yr (Bluth et al., 1992). G3 requires increasing rates of injection, to 9.8 Tg for the BNU-ESM at 2069. As aerosol loading increases, its efficacy decreases as particles coalesce and fall out of the stratosphere faster, while also becoming radiatively less effective (Niemeier and Timmreck, 2015). ~~Thus it seems that the disappearance of at least 1/3 of the glaciated area in HMA by 2069 cannot be prevented by sulphate aerosol geoengineering~~ This effect is so strong that it appears unfeasible to use sulphate aerosols to completely eliminate warming from scenarios such as RCP8.5. Greenhouse gas emissions would require very drastic reduction from present levels, and net negative emissions within the next few decades, to limit global temperature rises to 1.5 or 2°C (Rogelj et al., 2015). If such targets were met, then it is conceivable that plausible quantities of sulphate aerosol geoengineering may be able to maintain 2020 temperatures throughout the 21st century. Even if this politically very difficult combination of drastic emission cuts and quite aggressive sulphate aerosol geoengineering were done, then our simulations suggest the disappearance of about 1/3 of the glaciated area in HMA by 2069 still cannot be avoided.

## Acknowledgements

We thanks 2 anonymous referees for very constructive critiques of the paper, all participants of the Geoengineering Model Intercomparison Project and their model development teams, CLIVAR/WCRP Working Group on Coupled Modeling for endorsing GeoMIP, and the scientists managing the Earth System Grid data nodes who have assisted with making GeoMIP output available This study is supported by National Key Science Program for Global Change Research (2015CB953601), and National Natural Science Foundation of China (~~No~~Nos. 41530748, 41506212, 40905047).

## References

Arendt, A., et al.: Randolph Glacier Inventory - A Dataset of Global Glacier Outlines: Version 5.0. (GLIMS Technical Report) Global Land Ice Measurements from

---

Space, Boulder CO. Digital media, 2015.

835 Arora, V.K., et al.: Carbon emission limits required to satisfy future representative concentration pathways of greenhouse gases, *Geophys. Res. Lett.*, 38(5), L05805, 2011.

Azam, M.F., Wagnon, P., Ramanathan, A., Vincent, C., Sharma, P., Arnaud, Y., Linda, A., Pottakkal, G.J., Chevallier, P., Singh, V.B., and Berthier, E.: From balance to  
840 imbalance: a shift in the dynamic behaviour of Chhota Shigri Glacier (Western Himalaya, India), *J. Glaciol.*, 58 (208), 315–324, 2012.

Applegate, P.J. and Keller, K.: How effective is albedo modification (solar radiation management geoengineering) in preventing sea-level rise from the Greenland Ice Sheet? *Environ. Res. Lett.*, 10, 084018, 2015.

845 [Bahr, D. B., Meier, M., and Peckham, S.: The physical basis of glacier volume-area scaling, \*J. Geophys. Res.\*, 102, 355–362, 1997.](#)

[Becker, A., Finger, P., Meyer-Christoffer, A., Rudolf, B., Schamm, K., Schneider, U., and Ziese, M.: A description of the global land-surface precipitation data products of the Global Precipitation Climatology Centre with sample applications including centennial \(trend\) analysis from 1901–present, \*Earth Syst. Sci. Data\*, 5, 71–99, 2013.](#)  
850

Bluth, G.J.S., Doiron, S.D., Schnetzler, C.C., Krueger, A.J., and Walter, L.S.: Global tracking of the SO<sub>2</sub> clouds from the June 1991 Mount Pinatubo eruptions, *Geophys. Res. Lett.*, 19, 151–154, 1992.

855 Collins, W.J., et al.: Development and evaluation of an earth-system model-HadGEM2, *Geoscience Model Development*, 4, 1051–1075, 2011.

Dufresne, J.-L., et al.: Climate change projections using the IPSL-CM5 earth system model: From CMIP3 to CMIP5, *Clim. Dyn.*, 40, 2123–2165, 2013.

Du, J., He, Y., Li, S., Wang, S., Niu, H., Xin, H., and Pu, T.: Mass balance and near-  
860 surface ice temperature structure of Baishui Glacier No.1 in Mt. Yulong, *Journal of Geographical Sciences*, 23 (4), 668–678, 2013.

[Fujita, K. and Ageta, Y.: Effect of summer accumulation on glacier mass balance on the Tibetan Plateau revealed by mass-balance model, \*J. Glaciol.\*, 46\(153\), 244–252, doi:10.3189/172756500781832945, 2000.](#)

865 [Fujita, K. and Nuimura, T.: Spatially heterogeneous wastage of Himalayan glaciers, \*P. Natl. Acad. Sci. USA\*, 108, 14011 – 14014, doi:10.1073/pnas.1106242108, 2011.](#)

Gao, X., Shi, Y., Zhang, D., and Giorgi, F.: Climate change in China in the 21st century as simulated by a high resolution regional climate model, *Chin. Sci. Bull.*, 57, 1188–1195, 2012.

870 [Harris, I., Jones, P. D., Osborn, T. J., and Lister, D.H.: Updated high-resolution grids of monthly climatic observations – the CRU TS3.10 Dataset, \*Int. J. Climatol.\*, 34, 623–642, 2014.](#)

Irvine, P.J., Lunt, D.J., Stone, E.J., and Ridgwell, A.J.: The fate of the Greenland Ice Sheet in a geoengineered, high CO<sub>2</sub> world, *Environ. Res. Lett.*, 4, 045109, 2009.

875 Irvine, P.J., Striver, R.L., and Keller, K.: Tension between reducing sea-level rise and global warming through solar radiation management, *Nat. Clim. Change*, 2, 97–100, 2012.

- Ji, D., et al.: Description and basic evaluation of Beijing Normal University Earth System Model (BNU-ESM) version 1, Geoscientific Model Development, 7, 2039–2064, 2014.
- Jones, A., Haywood, J.M., Alterskjaer, K., Boucher, O., Cole, J.N.S., Curry, C.L., Irvine, P.J., Ji, D., Kravitz, B., Kristjánsson, J.E., Moore, J.C., Niemeier, U., Robock, A., Schmidt, H., Singh, B., Tilmes, S., Watanabe, S., and Yoon, J.-H.: The impact of abrupt suspension of solar radiation management (termination effect) in experiment G2 of the Geoengineering Model Intercomparison Project (GeoMIP), J. Geophys. Res. Atmos., 118 (17), 9743–9752, 2013.
- Johannesson, T., Raymond, C., and Waddington, E.: Time-scale for adjustment of glaciers to changes in mass balance, J. Glaciol., 35, 355–369, 1989.
- Kravitz, B., A. Robock, O. Boucher, H. Schmidt, K. E. Taylor, G. Stenchikov, and M. Schulz, The Geoengineering Model Intercomparison Project (GeoMIP), Atmos. Sci. Lett., 12(2), 162–167, 2011.
- Liu, X. and Chen, B.: Climatic warming in the Tibetan Plateau during recent decades, Int. J. Climatol. 20: 1729–1742, 2000.
- Luo, L.H., Zhang, Y.N., Zhou, J., Pan, X.D., and Sun, W.J., Simulation and Application of the Land Surface Model CLM Driven by WRF in the Tibetan Plateau, J. Glaciol. Geocryol., 35(3):553-564, 2013 (in Chinese with English abstract).
- Marzeion, B., Jarosch, A.H., and Hofer, M.: Past and future sea-level change from the surface mass balance of glaciers, Cryosphere 6, 1295–1322, 2012.
- McCusker, K.E., Battisti, D.S., and Bitz, C.M.: Inability of stratospheric sulfate aerosol injections to preserve the West Antarctic Ice Sheet, Geophys. Res. Lett., 42, 4989–4997, 2015.
- Maussion, F., Scherer, D., Mdg, T., Collier, E., Curio, J., Finkelnburg, R., Precipitation seasonality and variability over the Tibetan Plateau as Resolved by the High Asia Reanalysis, J. Climate, 27, 1910-1927, 2014.
- Mdg, T., Maussion, F., and Scherer, D., Mid-latitude westerlies as a driver of glacier variability in monsoonal High Asia, Nat. Clim. Change, 4, 68-73, 2014.
- Mdg, T., Maussion, F., Yang, W., and Scherer, D.: The footprint of Asian monsoon dynamics in the mass and energy balance of a Tibetan glacier, Cryosphere 6, 1445–1461, 2012.
- Moore, J.C., Jevrejeva, S., and Grinsted, A.: Efficacy of geoengineering to limit 21st century sea-level rise, Proc. Natl. Acad. Sci., 107, 15699–15703, 2010.–
- Moore J.C., Grinsted, A., Zwinger, T., and Jevrejeva, S.: Semiempirical and process-based global sea level projections. Rev. Geophys., 51, 1 – 39, 2013.
- Niemeier, U. and Timmreck, C.: What is the limit of stratospheric sulfur climate engineering? Atmos. Chem. Phys. Discuss, 15, 10939–10969, 2015.
- Nuimura T., A. Sakai, K. Taniguchi, H. Nagai, D. Lamsal, S. Tsutaki, A. Kozawa, Y. Hoshina, S. Takenaka, S. Omiya, K. Tsunematsu, P. Tshering, and K. Fujita: The GAMDAM Glacier Inventory: a quality controlled inventory of Asian glaciers. Cryosphere, 9, 849 – 864, 2015 (doi: 10.5194/tc-9-849-2015)
- Pu, J., T. Y., Duan, K., Sakai, A., Fujita, K., and Matsuda, Y.: Mass balance of the Qiyi Glacier in the Qilian Mountains: a new observation (in Chinese with English

- abstract), J. Glaciol. Geocryol. 27, 199–204, 2005.
- Ricke, K.L., Morgan, M.G., and Allen, M.R.: Regional climate response to solar-radiation management, Nat. Geosci., 3, 537–541, 2010.
- 925 [Radic, V., Hock, R., and Oerlemans, J.: Analysis of scaling methods in deriving future volume evolutions of valley glaciers, J. Glaciol., 54, 601–612, 2008.](#)
- Radić, V., Bliss, A., Beedlow, A.C., Hock, R., Miles, E., and Cogley, J.G.: Regional and global projections of the 21st century glacier mass changes in response to climate scenarios from GCMs. Clim. Dyn., 42, 37–58, 2014.
- 930 [Rogelj, J., Luderer, G., Pietzcker, R.C., Kriegler, E., Schaeffer, M., Krey, V., Riahi, K.: Energy system transformations for limiting end-of-century warming to below 1.5 °C. Nature Climate Change \(doi: 10.1038/NCLIMATE2572\). 2015.](#)
- Rupper, S. and Roe, G.: Glacier changes and regional climate: a mass and energy balance approach, J. Clim., 21, 5384–5401, 2008.
- 935 Taylor, K.E., Stouffer, R.J., and Meehl, G.A.: An overview of CMIP5 and the experiment design, Bulletin of the American Meteorological Society, 93, 485–498, 2012.
- Tilmes, S., et al.: The hydrological impact of geo-engineering in the Geoengineering Model Intercomparison Project (GeoMIP), J. Geophys. Res., 118(19), 11036–11058, 2013.
- 940 [van de Berg, W. J., van den Broeke, M., Ettema, J., van Meijgaard, E., and Kaspar, F., Significant contribution of insolation to Eemian melting of the Greenland ice sheet, Nature Geosci. 4\(10\), 679–683, 2011.](#)
- Wagnon, P., Linda, A., Arnaud, Y., Kumar, R., Sharma, P., Vincent, C., Pottakkal, G.J., Berthier, E., Ramanathan, A., Hasnain, S.I., and Chevallier, P.: Four years of mass balance on Chhota Shigri Glacier, Himachal Pradesh, India, a new benchmark glacier in the Western Himalaya, J. Glaciol., 53 (183), 603–610, 2007.
- 945 Wang S., Pu J., and Wang N.: Study of Mass Balance and Sensibility to Climate Change of Qiyi Glacier in Qilian Mountains (in Chinese with English abstract), J. Glaciol. Geocryol., 33(06), 1214–1221, 2011.
- 950 Watanabe, S., et al.: MIROC-ESM 2010: Model description and basic results of CMIP5-20c3m experiments. Geoscience Model Development 4, 845–872, 2011.
- WGMS: Glacier Mass Balance Bulletin No. 1 (1988-1989), ed. Haeberli, W., and E. Herren. IAHS (ICSU)/UNEP/UNESCO, World Glacier Monitoring Service, Zurich, 1991.
- 955 WGMS: Glacier Mass Balance Bulletin No. 2 (1990-1991), ed. Haeberli, W., E. Herren and M. Hoelzle. IAHS (ICSU)/UNEP/UNESCO, World Glacier Monitoring Service, Zurich, 1993.
- WGMS: Glacier Mass Balance Bulletin No. 3 (1992-1993), ed. Haeberli, W., M. Hoelzle and H. Bosch. IAHS (ICSU)/UNEP/UNESCO, World Glacier Monitoring Service, Zurich, 1994.
- 960 WGMS: Glacier Mass Balance Bulletin No. 4 (1994-1995), ed. Haeberli, W., M. Hoelzle and S. Suter. IAHS (ICSU)/UNEP/UNESCO, World Glacier Monitoring Service, Zurich, 1996.
- 965 WGMS: Glacier Mass Balance Bulletin No. 5 (1996-1997), ed. Haeberli, W., M.



---

Hoelzle and R. Frauenfelder. IAHS (ICSU)/UNEP/UNESCO, World Glacier Monitoring Service, Zurich, 1999.

WGMS: Glacier Mass Balance Bulletin No. 6 (1998-1999), ed. Haeberli, W., R. Frauenfelder and M. Hoelzle. IAHS (ICSU)/UNEP/UNESCO/WMO, World Glacier Monitoring Service, Zurich. WGMS. 2003. Glacier Mass Balance Bulletin No. 7 (2000-2001), ed. Haeberli, W., R. Frauenfelder, M. Hoelzle and M. Zemp. IAHS (ICSU)/UNEP/UNESCO/WMO, World Glacier Monitoring Service, Zurich, 2001.

WGMS: Glacier Mass Balance Bulletin No. 8 (2002-2003), ed. Haeberli, W., J. Noetzli, M. Zemp, S. Baumann, R. Frauenfelder and M. Hoelzle. IUGG (CCS)/UNEP/UNESCO/WMO, World Glacier Monitoring Service, Zurich, 2005.

WGMS: Glacier Mass Balance Bulletin No. 9 (2004-2005), ed. Haeberli, W., M. Hoelzle and M. Zemp. ICSU (FAGS)/IUGG (CCS)/UNEP/UNESCO/WMO, World Glacier Monitoring Service, Zurich, 2007.

WGMS: Glacier Mass Balance Bulletin No. 10 (2006-2007), ed. Haeberli, W., I. Gärtner-Roer, M. Hoelzle, F. Paul and M. Zemp. ICSU (WDS)/IUGG (IACS)/UNEP/UNESCO/WMO, World Glacier Monitoring Service, Zurich, 2009.

WGMS: Glacier Mass Balance Bulletin No. 11 (2008-2009), ed. M. Zemp, S. U. Nussbaumer, I. Gärtner-Roer, M. Hoelzle, F. Paul and W. Haeberli. ICSU (WDS)/IUGG (IACS)/UNEP/UNESCO/WMO, World Glacier Monitoring Service, Zurich, 2011.

WGMS: Glacier Mass Balance Bulletin No. 12 (2010-2011), ed. M. Zemp, S. U. Nussbaumer, K. Naegeli, I. Gärtner-Roer, F. Paul, M. Hoelzle and W. Haeberli. ICSU (WDS)/IUGG (IACS)/UNEP/UNESCO/WMO, World Glacier Monitoring Service, Zurich, 2013.

Yang, W., Yao, T., Guo, X., Zhu, M., Li, S., and Kattel, D. B.: Different region climate regimes and topography affect the changes in area and mass balance of glaciers on the north and south slopes of the same glacierized massif (the West Nyainqentanglha Range, Tibetan Plateau), *Journal of Hydrology* 495, 64-73, 2013.

Yao, T., Thompson, L., Yang, W., Yu, W., Gao, Y., Guo, X., Yang, X., Zhao, H., Duan, K., Xu, B., Pu, J., Lu, A., Qin, D.H., Xiang, Y., Kattel, D.B., and Joswiak, D.: Different glacier status with atmospheric circulations in Tibetan Plateau and surroundings, *Nat. Clim. Chang.* 15, 2012, <http://dx.doi.org/10.1038/NCLIMATE1580> (supplementary information).

Yang, W. and T. Yao, et al.: Mass balance of a maritime glacier on the southeast Tibetan Plateau and its climatic sensitivity, *J. Geophys. Res. Atmos.*, 118 (17), 9579-9594, 2013.

Yu, X., Moore, J. C., Cui, X., Rinke, A., Ji, D., Kravitz, B. and Yoon J.-H.: Impacts, effectiveness and regional inequalities of the GeoMIP G1 to G4 solar radiation management scenarios, *Global Planet. Change*, 129, 10–22, 2015.

Yu, W., Yao, T., Kang, S., Pu, J., Yang, W., Gao, T., Zhao, H., Zhou, H., Li, S., Wang, W., Ma, L., Different region climate regimes and topography affect the changes in area and mass balance of glaciers on the north and south slopes of the same glacierized massif (the West Nyainqentanglha Range, Tibetan Plateau), *J. Hydrol.*,

495, 64 - 73, 2013.

Zhang, J., He, X., Ye, B., et al.: Recent Variation of Mass Balance of the Xiao Dongkemadi Glacier in the Tanggula Range and its influencing factors (in Chinese with English abstract), J. Glaciol. Geocryol., 35(2), 263-271, 2013.

Zhang, H., Li, Z., Wang, P., and Huai, B.: Variation of Haxilegen No.51 Glacier at the Headwater of Kuytun River in Tianshan Mountains and Its Response to Climate Change, Arid Zone Research, 32(1), 88-93, 2015.

Zhou, G., Yao, T., Kang, S., Pu, J., Tian, L., and Yang, W.: Mass balance of the Zhadang Glacier in the central Tibetan Plateau (in Chinese with English abstract). J. Glaciol. Geocryol. 29 (3), 360–365, 2007.

Zhao, L., Ding, R., and Moore, J.C.: Glacier volume and area change by 2050 in high mountain Asia, Global Planet. Change, 122, 197-207, 2014.

Zhao, L., Ding, R., and Moore, J.C.: The High Mountain Asia glacier contribution to sea level rise from 2000 to 2050, Ann. Glaciol., 71, 223-231, 2016.

Table 1. The benchmark glaciers, their RGI 5.0 sub-regions, and their exact location (Fig. 1), altitude range, averaged SMB gradients (unit:  $\text{m m}^{-1}$ ) is specific altitude intervals, ELA and SMB data sources.

Glacier name and Sub-region	Location Sub-region	Altitude range (m)	Averaged SMB gradients	Period of SMB measurements	Reference
Abramov Glacier (13-01)	<del>(39°38'N, 71°36'E)</del> 01	<del>3600-4700(39°38'N, 71°36'E)</del> 3600-4700	0, $z > \text{ELA} + 200$ ; 0.0088, $z < \text{ELA} + 200$ . <u>ELA varies in 4050-4450</u>	1987-1997	Glacier mass balance bulletin No. 1-6.
Ts. Tuyuksuyskiy Glacier (13-03)	<del>(43°03'N, 77°05'E)</del> 03	<del>3400-4200(43°03'N, 77°05'E)</del> 3400-4200	0, $z > \text{ELA} + 100$ ; 0.0057, $z < \text{ELA} + 100$ . <u>ELA varies in 3600-4200</u>	1987-2011	Glacier mass balance bulletin No. 1-12.
Urumqihe S. No.1 Glacier (13-04) (East branch)	<del>(43°06'N, 86°49'E)</del> 04	<del>3700-4300(43°06'N, 86°49'E)</del> 3700-4300	0.002, ELA $< z < 4300$ ; 0.01, $z < \text{ELA}$ . <u>ELA varies in 3950-4175</u>	1987-2011	Glacier mass balance bulletin No. 1-12.
Haxilegen No.51 Glacier (13-04)	<del>84°24'E, 43°43'N</del> 04	<del>3475-3700(84°24'E, 43°43'N)</del> 3475-3700	0.012	1999-2005	Zhang et al. (2015)
Qiyi Glacier (13-07)	<del>(39°14'N, 97°45'E)</del> 07	<del>4310-5145(39°14'N, 97°45'E)</del> 4310-5145	0.0042, 4800 $< z < \text{ELA}$ ; 0.0014, $z < 4800$ . <u>where ELA=5012</u>	2002 Jun-Sep; 2002-03; 2010	Pu et al. (2005); Wang et al.(2011)
Zhadang Glacier (13-08)	<del>(30°28'N, 90°38'E)</del> 08	<del>5515-6090(30°28'N, 90°38'E)</del> 5515-6090	0.0041	2005-06; 2009 Jun-Jul; 2009 Sep- <u>2010 May 2010</u> <u>May;</u>	Zhou et al.(2007), Mǎg et al. (2012). Yu et al. (2013)

				2010 Aug-Sep	
Gurenhekou	13-	(30°11'N,90°27'E	0.0041	2004-08	Yu et al. (2013)
Glacier (13-08)	08	(30°11'N	5550-6020		
		90°27'E)			
Xiao Dongkemadi	(33 04 N,	5380-	0.007, z<ELA;	2008-12	Zhang et al. 2013)
Glacier (13-08)	92 05 E)13-	5926(33 04 N,	0.004, ELA<z<5750		
	08	92 05 E)	where ELA~5515		
Chhota Shigri	(32 12 N,	4000-	0.003, ELA<z<5600;	Annual average	Azam et al. (2012);
Glacier (14-03)	77 30 E)14-	5600(32 12 N,	0.01,	SMB during	Wagnon et al.
	03	77 30 E)	ELA-150<z<ELA;	2002-10;	(2007)
			0.005,	2003-04;	
			4000<z<ELA-150	2004-05	
			where ELA varies in 4855-		
			5180		
Naimona'nyi	(30 27 N,	5600-	0.0006, z>ELA;	2005-2010	Yao et al. (2012)
Glacier (15-01)	81 20 E)15-	6150(30 27 N,	0.0038, 5700<z<ELA;		
	01	81 20 E)	where ELA~6100		
Kangwure Glacier	(28 28 N,	5700-	0.0038, 5700<z<6100;	2005-2010	Yao et al. (2012)
(15-01)	85 49 E)15-	6100(28 28 N,			
	01	85 49 E)			
Parlung No.94	(29 20 N,	5067-	0.01	2006-10	Yang et al. (2013)
Glacier (15-03)	97 0'E)15-	5334(29 20 N,			
	03	97 0'E)			
Baishui No.1	26°59'-27°	4300-	0.003,z>ELA	2008-09	Du et al. (2013)
Glacier (15-03)	17'N,	500026°59'-27°1	0.01,		
	100°04'-10	7'N,	ELA-250<z <ELA;		
	0°15'E)15-	100°04'-100°15'E	0.0035,		
	03		4300<z<4650		
			where ELA =4972		

1030

Table 2 GriddedThe average rate of elevation change ( $\text{m a}^{-1}$ ) for all the glaciers in sub-regions compared with remote-sensing estimates from 2003 to 2009 from Gardner and others (2013).

Sub-regions	Gardner and others (2013)	Modelled
Hissar Alay and Pamir	-0.13±0.22	-0.02±0.49
S and E Tibet	-0.30±0.13	-0.39±0.75
Hindu Kush and	-0.12±0.15	-0.08±0.29
Karakoram		
W Himalaya	-0.53±0.13	0.32±0.29
C Himalaya	-0.44±0.20	-0.62±0.63
E Himalaya	-0.89±0.18	-1.51±0.59
All HMA	-0.27±0.17	-0.13±0.60

1035

**Table 3** climate ~~data sets~~ **models and datasets** used in this study.

Name	Reference	Resolution	Data sets
<del>Berkeley Earth project</del>	<del>RohdeHarris et al., 2013</del>	<del>1°×10.5°×0.5°</del>	Surface temperature 1980-2013
<del>GPCC</del>	<del>Becker et al., 2013</del>	<del>0.5°×0.5°</del>	<del>Precipitation 1980-2013</del>
BNU-ESM	Ji et al., 2014	2.8°×2.8°	G3,G4, RCP4.5, RCP8.5
CanESM2	Arora et al., 2011	2.8°×2.8°	G4, RCP4.5, RCP8.5
HadGEM2-ES	Collins et al., 2011	1°×1.9°	G3,G4, RCP4.5, RCP8.5
IPSL-CM5A-LR	Dufresne et al., 2013	1.9°×3.8°	G3, RCP4.5, RCP8.5
MIROC-ESM	Watanabe et al., 2011	2.8°×2.8°	G4, RCP4.5, RCP8.5
MIROC-ESM-CHEM	Watanabe et al., 2011	2.8°×2.8°	G4, RCP4.5, RCP8.5

**Table 3.** ~~Mean and standard deviation of mean surface air temperature and precipitation anomalies averaged over the whole study region during 2030–2069 simulated from G3, G4, RCP4.5 and RCP8.5 ensembles (Table 2). Anomalies are relative to the baseline RCP4.5 climate state between 2010 and 2029.~~

**Table 4.** The volume loss in mm sea-level equivalent, projected using forcing from all the climate models in the period 2010-2069 and 2070-2089 post-geoengineering period under G3, G4, RCP4.5 and RCP8.5. The means of volumes lost driven by individual model forcing and its standard deviation are shown in the penultimate row. The simulated volume loss using the climate model ensemble mean forcing of temperature and precipitation is shown in the last row. The volume loss is calculated by assuming ice density of 900 kg m<sup>-3</sup> and ocean area of 362×10<sup>12</sup> m<sup>2</sup>.

EnsembleScenari	$-\Delta T(^{\circ}C)_{G3}$		$-\Delta P(mm\ day^{-1})_{G4}$		RCP4.5		RCP8.5	
os								
Period	2010-69	2070-89	2010-69	2070-89	2010-69	2070-89	2010-69	2070-89
Model	69	-89						
BNU-ESM	10.2	5.3	11.0	5.5	18.5	2.5	20.8	3.2
G3CanESM2	----	----	8.3	4.1	14.0.17±0.1	2.0.01±0.0	17.8	3.5
					8	7		
HadGEM2-ES	7.2	3.4	3.2 <sup>E</sup>	3.7 <sup>E</sup>	12.0	2.5	15.9	4.7
IPSL-CM5A-LR	9.8	6.3	----	----	16.7	3.2	19.5	3.8
G4MIROC-ESM	----	----	12.6	4.0.50±0.3	15.8	3.0.05±0.0	19.0	3.9
				4		8		
RCP4.5MIROC-ESM-CHEM	----	----	1.30±14.0.34	3.8	16.0.07±0.1	2.9	19.1	3.1
					0			
Mean ± std	9.0±1.6	5.4 ± 1.0	RCP811.5±2.5	4.4±0.8	15.5±2.3	2.037 ± 0.464	18.5±1.7	3.7 ± 0.09±0.13
							6	
Ensemble mean	8.1	5.9	11.7	4.7	16.6	2.9	19.2	3.6

---

---

climate forcing

---

<sup>‡</sup>HadGEM2-ES is excluded from the mean of the models in G4